Title

Disentangling Landscape Heterogeneity: Compositional, Configurational, Vertical, and Temporal Heterogeneity

Soyeon Bae [a], Catrin Westphal [a,b], Christian Ammer [a,c], Patrick Hostert [d], Silke Hüttel [e], Krisztina Kis-Katos [f], Thomas Kneib [g], Holger Kreft [a,h], Carola Paul [a,i], Tobias Plieninger [j], Birgitta Putzenlechner [a], Reimund Rötter [a,k], Michael Schlund [l], Dominik Seidel [a,m], Stefan Siebert [n], Kerstin Wiegand [a,o], Alexander Knohl [a,p]

Affiliations:

a) Centre of Biodiversity and Sustainable Land Use, University of Göttingen, Göttingen, Germany
b) Functional Agrobiodiversity & Agroecology, Department of Crop Sciences, University of Göttingen, Göttingen, Germany
c) Silviculture and Forest Ecology of the Temperate Zones, University of Göttingen, Göttingen, Germany
d) Earth Observation Lab, Geography Department, Humboldt-Universität zu Berlin, Germany
e) Management in Agricultural and Food Economics, Department of Agricultural Economics and Rural Development, University of Göttingen, Göttingen, Germany
f) International Economic Policy, Department of Economics, University of Göttingen, Göttingen, Germany
g) Chair of Statistics, Faculty of Mathematics and Computer Science, University of Göttingen, Göttingen, Germany

h) Biodiversity, Macroecology & Biogeography, University of Göttingen, Göttingen, Germany
i) Forest Economics and Sustainable Land-use Planning, University of Göttingen, Göttingen, Germany
j) Social-Ecological Interactions in Agricultural Systems, University of Göttingen and University of Kassel, Germany
k) Tropical Plant Production and Agricultural Systems Modelling (TROPAGS), University of Göttingen, Göttingen, Germany
l) Department of Natural Resources, Faculty of Geo-information Science and Earth Observation (ITC), University of Twente, The Netherlands
m) Spatial Structures and Digitization of Forest, University of Göttingen, Göttingen, Germany
n) Chair of Agronomy, Department of Crop Sciences, University of Göttingen, Göttingen, Germany
o) Ecosystem Modelling, Büsgen-Institute, University of Göttingen, Göttingen, Germany
p) Bioclimatology, University of Göttingen, Göttingen, Germany

***Correspondence**: Soyeon Bae, soyeon.bae@uni-goettingen.de**,** ORCID iD: 0000-0003-1961-1226

Acknowledgements

This work was supported by the Lower Saxony Ministry of Science and Culture and the VolkswagenStiftung through the program "ExzellenzStärken". We thank Miriam Teuscher, Liv Kalbitzer, and Sandra Schweiger for their support in project coordination, and Elisabeth Dietze, Dirk Hölscher, Johannes Kamp, Daniela Sauer, and Fabian Sinz for their constructive feedback on the analysis. CW is grateful for funding by the Deutsche Forschungsgemeinschaft (DFG, German Research Foundation, project number 493487387). PH acknowledges funding for GreenGrass II by the German Federal Ministry of Education and Research (BMBF), project number 031B1526J.

Conflict of Interest Statement.

The authors have no competing interests to declare.

Abstract and keywords

Aim

Landscape heterogeneity is a key driver of biodiversity, ecosystem functioning, and resilience. However, the complex relationships among different components of heterogeneity—compositional, configurational, vertical, and temporal—remain underexplored for large areas such as at the national scale. This study examines the associations among multiple landscape heterogeneity components across land-cover types to refine their use in ecological research.

Location

Germany

Time Period

Mainly 2017-2020

Major Taxa Studied

Not taxa-specific; focuses on landscape heterogeneity as an ecological driver.

Methods

We analysed nationwide spatial datasets at very high resolution (10–30 m resolution) of land-cover types, dominant tree species, canopy height, and time-series of crop types as well as grassland mowing frequency. We applied Structural Equation Modeling (SEM) to assess the statistical relationship between heterogeneity indices and their interactions. Specifically, we examined (i) compositional vs. configurational heterogeneity (i.e., Shannon diversity vs. edge density), (ii) configurational heterogeneity vs. connectivity, (iii) horizontal vs. vertical and temporal heterogeneities, and (iv) heterogeneities across multiple land-cover types based on grid cells of 3 x 3 km^2.

Results

Our findings reveal that compositional and configurational heterogeneities exhibit positive correlations, but their relationships are moderated by the proportions of land-cover types. Configurational heterogeneity does not enhance connectivity; after controlling for land-cover proportions, its partial association with connectivity is negative. Vertical and temporal heterogeneities show limited associations with horizontal compositional and configurational heterogeneities, suggesting relative independence. Principal component analysis indicates that landscape heterogeneity is primarily driven by heterogeneities of forest and overall land-cover, e.g., edge densities of forest dominant tree species and overall land-cover types, whereas cropland heterogeneity, e.g., Shannon diversity of crop types, contributes negatively.

Main Conclusions

Our study underscores the importance of accounting for land-cover proportions when analysing landscape heterogeneity relationships. Failing to do so can distort the model due to potential hidden collinearity. Additionally, our findings highlight the need to capture the multi-dimensional nature of landscape heterogeneity in biodiversity and ecosystem studies. Landscape heterogeneity is shaped by the interdependencies between prevailing land-cover patterns, likely influenced by land-use decisions and history as well as social-ecological contexts, highlighting the need for cross-national or cross-administrative studies.

Keywords

compositional heterogeneity, configurational heterogeneity, connectivity, land-cover proportions, landscape heterogeneity, remote sensing, structural equation modelling, temporal heterogeneity, vertical heterogeneity.

Main text

1. Introduction

Landscape heterogeneity has been studied in biodiversity research for several decades and is regarded as a foundational characteristic essential for maintaining biodiversity (MacArthur and MacArthur 1961; Fahrig et al. 2011; Stein et al. 2014). More recently, landscape heterogeneity has also attracted attention for its role as a buffer against disturbances, potentially enhancing ecosystem resilience (Papanikolaou et al. 2017; Zhang et al. 2020; Seidel and Ammer 2023). As research has progressed, the effects of landscape heterogeneity on biodiversity have been shown to vary across taxonomic groups, environmental domains (e.g., climate, topography, land-cover), and spatial scales (Stein et al. 2014; Heidrich et al. 2020).

The concept has evolved from a focus on compositional heterogeneity— the number and proportions of different elements—to also encompass configurational heterogeneity, referring to the spatial arrangement and shape of those elements (Fahrig et al. 2011); we refer to these as two core attributes of landscape heterogeneity in this study (Fig. 1). In parallel, the study of landscape heterogeneity in complex ecosystems has grown more sophisticated, expanding from two-dimensional (2-D) to three-dimensional (3-D) perspectives and, more recently, to include the temporal dimension. This shift has been facilitated by advances in scientific and technical tools, particularly remote sensing (Davies and Asner 2014; Coops et al. 2019; Torresani et al. 2023). Although landscape heterogeneity has traditionally been defined as the spatial heterogeneity of landscape features such as land-cover types, vegetation composition and physiognomy, and abiotic factors (Stein et al. 2014), we expand this definition to include temporal heterogeneity in response to the growing interest in its ecological relevance (Allan et al. 2014; Schellhorn et al. 2015; Coops et al. 2019; Fijen et al. 2025) (Fig. 1).

Given the expansion in our understanding of landscape heterogeneity, it is becoming increasingly important to understand the unique effects of each component of landscape heterogeneity on ecosystem function, disentangling multiple forms of heterogeneity in complex landscapes. In biodiversity research, disentangling configurational and compositional heterogeneity has become increasingly important, as they have been shown to play distinct roles in shaping animal communities. For instance, these two attributes of heterogeneity filter different arthropod traits and help mitigate biotic homogenisation (Gámez-Virués et al. 2015). Configurational heterogeneity has also shown strong positive effects on trait dominance within communities, while compositional heterogeneity had strong positive effects on taxonomic diversity (Perović et al. 2015). Additionally, configurational heterogeneity is receiving more attention for its potential to enhance ecosystem resilience, for example, in regard to pests (Zhang et al. 2020).

In terms of the dimension expansion of landscape heterogeneity, the development of remote sensing technologies, such as airborne LiDAR (Light Detection and Ranging), SAR (Synthetic Aperture Radar), and UAV (Unmanned Aerial Vehicles) photogrammetry, have illuminated the effects of 3-D heterogeneity on biodiversity over the past two decades, from forest habitats to grasslands (Davies and Asner 2014; Bae et al. 2019; Torresani et al. 2024). Over the last decade, high-resolution satellite data, such as Sentinel-1 and Sentinel-2, now allow creating time-series of national maps depicting landscape features, e.g. dominant tree species, crop types, crop rotation or mowing frequency (Schwieder et al. 2022; Blickensdörfer et al. 2022, 2024). These maps facilitate the calculation of landscape heterogeneity within an individual land-cover type (e.g., crop type heterogeneity in croplands, dominant tree species heterogeneity in forests, mowing frequency heterogeneity in grasslands) at a national level, which was previously impossible based on field surveys or airborne data. Furthermore, multi-temporal maps enable the exploration of temporal heterogeneity—such as inter-annual heterogeneity in grassland mowing frequencies and crop sequences—although its effects on biodiversity are still to be understood in more detail. The impact of temporal heterogeneity on biodiversity is contentious, with some arguing for positive impacts due to increased temporal niche separation and diversification (Allan et al. 2014; Doležal et al. 2019; Fijen et al. 2025), while others suggest negative impacts due to decreased stability (Schellhorn et al. 2015; Coops et al. 2019).

In light of the growing interest in available data on landscape heterogeneity, exploring the relationships between the different components of heterogeneity and embracing the complexity of landscape heterogeneity can enhance its application in ecological studies. As a notable example, compositional and configurational heterogeneities have been assumed to be correlated, and it is recommended to select sampling points where both heterogeneities show less correlation from the outset of the study design (Fahrig et al. 2011; Pasher et al. 2013; Perović et al. 2015). The collinearity between these two heterogeneity variables has been tested in individual study areas to maintain statistical robustness (Perović et al. 2015; Gámez-Virués et al. 2015). Furthermore, as horizontal and vertical landscape heterogeneities can sometimes be highly correlated, previous studies have been cautious in their selection of variables to avoid collinearity (Jung et al. 2012; Heidrich et al. 2020). As such, due to possible correlations between diverse types of landscape heterogeneity, their relationships have been examined in individual study areas. However, to the best of our knowledge, the overall correlation patterns of landscape heterogeneity—across multiple dimensions, attributes, and land-cover types (see Fig. 1)—have not yet been systematically investigated at large spatial scales. Such research is essential for refining the selection of heterogeneity indices, informing site stratification, and accounting for key covariates or interactions in ecological analyses.

In this study, we explored the nationwide relationships among diverse components of landscape heterogeneity, both across all land-cover types (hereafter, LC) and within individual land-cover types—specifically forests, croplands, and grasslands. For the horizontal heterogeneity, we first examined the association between compositional and configurational heterogeneities —two core attributes of landscape heterogeneity. We then explored how both compositional and configurational heterogeneities relate to connectivity. While landscape connectivity is not a form of heterogeneity itself, configurational heterogeneity is often assumed to enhance landscape connectivity and is sometimes confused with it (Fahrig 2017; Estrada-Carmona et al. 2022). Thus, we explored whether configurational heterogeneity enhances landscape connectivity. We then assessed the strength of associations between horizontal heterogeneity and both vertical and temporal heterogeneities—representing additional dimensions of landscape heterogeneity. Finally, we examined how landscape heterogeneity across multiple land-cover types—for example, between forest-related and cropland-related heterogeneity—is interrelated. Utilising open-access data, we tested the relationships between heterogeneities via correlation tests and Structural Equation Modelling (SEM). Based on the generally strong associations reported in the literature among different components of landscape heterogeneity, we assumed positive associations across all four types of comparisons.

In addition, abiotic factors such as topography and soil properties can influence land-use decisions and, in turn, the spatial distribution of land-cover types. For instance, regions with more productive soils may be associated with a higher proportion of cropland and a lower proportion of forest. The dominance of particular land-cover types—potentially shaped by such abiotic factors—can influence landscape heterogeneity. Likewise, land-cover proportions (hereafter % land-cover), which may significantly affect biodiversity, have been assumed to correlate with landscape heterogeneity (Fahrig 2017) and were recently shown to interact with configurational heterogeneity in relation to biodiversity (Martin et al. 2019). Thus, we included abiotic factors and % land-cover in our SEM as an intermediate variable in association chains to examine the partial relationships between heterogeneity variables and explore the potential role of % land-cover in mediating relationships (see Method section 2.3 for details). We hypothesised that the relationships among heterogeneity components may also depend on their associations with % land-cover.

2. Materials and methods

2.1. Study area

This study was conducted across Germany, covering approximately 357,000 km², with elevations ranging from 0 m to about 2,900 m a.s.l. The land cover comprises 35.8% forest, 32.6% cropland, and 22.4% grassland, with the remaining area distributed among categories such as artificial land, wetlands, and water bodies (Fig. S1) Recent biodiversity studies in Germany analysing landscape-scale effects tested plot-diameters between 1 and 6 km, with 2 or 4 km proving most effective in explaining ecological responses (Gámez-Virués et al. 2015; Seibold et al. 2019; Fricke et al. 2022; Le Provost et al. 2022). Based on these findings, we divided Germany into 41,060 grid cells of 3 x 3 km² for statistical analyses of landscape heterogeneity.

2.2. Data source and calculation of heterogeneity

Germany-wide spatially explicit data on land cover and land management practice were used. These included satellite-derived maps (10-30 m resolution) for land cover (Pflugmacher et al. 2018), crop types (Blickensdörfer et al. 2022), dominant forest tree species (Blickensdörfer et al. 2024), grassland mowing frequency (Schwieder et al. 2022), and canopy height (Lang et al. 2022). Additionally, agricultural census data on average farm size at a 5 km resolution (Federal Statistical Office and the statistical offices of the Länder 2020) were incorporated (Fig. 2).

Compositional heterogeneity was quantified using the *Shannon* diversity index (*H'*) for categorical data and standard deviation for numerical data. Configurational heterogeneity was assessed via edge density (ED) and average size (Table 1; Note S1 for equations of *H'* and *ED*). Temporal heterogeneity was derived from available yearly time-series maps, i.e., crop type and mowing frequency maps (2017-2020). Temporal compositional heterogeneity was calculated using *H'* across four years, while temporal configurational heterogeneity was determined using the interannual change rate (Fig. S2). We could not capture all components of landscape heterogeneity due to limited or unsuitable data for certain aspects. For example, compositional heterogeneity of numerical variables such as mowing frequency and canopy height was assessed using standard deviation. However, we considered it inappropriate to derive configurational heterogeneity from these variables.

Woody vegetation and grassland connectivity were each assessed using dedicated connectivity indices. Woody vegetation connectivity was calculated by combining forest areas (Blickensdörfer et al. 2024) with small woody features derived from the crop type map (Blickensdörfer et al. 2022), treating them as habitat patches for the connectivity index. Grassland connectivity was assessed using all grassland areas identified from mowing frequency maps (Schwieder et al. 2022), which served as habitat patches in the connectivity analysis. Connectivity was calculated in each 3 x 3 km grid cell using *Graphab* (R package *graph4lg*). Habitat patches were connected using Euclidean distances and nearest-neighbour relationships, providing a practical approximation of a fully connected network (see details in Fig. S3). Connectivity was quantified using the Equivalent Connectivity index, calculated as the square root of the summed product of patch areas weighted by interaction probability (Saura et al. 2011). This index allows for intuitive interpretation, as it is expressed in area units and can be directly compared to the size of a single habitat patch that would provide an equivalent level of connectivity. The Equivalent Connectivity index was then computed:

$$\text{Equivalent Connectivity} = \sqrt{\sum_{i=1}^{n}\sum_{j=1}^{n} a_i a_j e^{-\alpha d_{ij}}}$$

n is the number of patches, a_i is the area of the patch i, d_{ij} is the distance between patches i and j, and $e^{-\alpha d_{ij}}$ is the probability of movement between the patches i and j. The parameter α is defined as the rate of decline in probability when distance increases, calculated as $-\log(p_{min})/_{d_{max}}$, where p_{min} is the minimum probability of movement with the default value of 0.05 at the maximum dispersal distance of species (d_{max}). Although specific species were not defined for the connectivity analysis, the selected threshold distance (d_{max}) of up to 3 km is ecologically relevant for several spore-dispersing groups—such as bryophytes, lichens, and fungi—as well as flying vertebrates like birds and bats, and large insects such as bumblebees. (Westphal et al. 2006; Abrego et al. 2018; Komonen and Müller 2018).

Abiotic factors potentially influencing % land-cover were collected, including topography (NASA Shuttle Radar Topography Mission (SRTM) 2013), soil texture and soil moisture (Hiederer 2013; Deutscher Wetterdienst (DWD) 2021), and climate data (Fick and Hijmans 2017) (see all abiotic factors before variable selection in Table S1). Following multicollinearity analysis, only slope and soil moisture were retained in the further analysis due to their strong correlation with % land-cover and low collinearity between each other (*Spearman*'s *rho* < 0.6). % Land-cover is calculated for each individual land-cover type and labeled accordingly; for example, *% forest* represents the proportion of forest cover.

2.3. Statistical analysis

Spearman's rank correlation was used to assess relationships among heterogeneity indices, as it is more robust than *Pearson*'s correlation and better captures nonlinear dependencies. To examine how % land-cover influences the relationship between *H'* and *ED*, quantile correlation tests were performed for deciles of % land-cover using *Spearman*'s correlation.

SEM quantified direct and indirect paths/relationships and residual covariance of relationships among abiotic factors, % land-cover, and multiple landscape heterogeneity components using the maximum likelihood method. SEM explores correlations within a defined network, including association chains, such as "A relates to B, which relates to C". This strength of SEM facilitates the measurement of indirect or cascading linkages. SEM estimates a partial regression coefficient (hereafter, path coefficient) that indicates the strength of a single predictor variable on the response while simultaneously considering the relations of other variables in the model (Grace and Keeley 2006). SEMs were used in this study to model the relationships (1) between compositional and configurational heterogeneities both across LC and within individual land-cover types—forests and croplands (see full variables and model in Fig. S5), (2) between configurational heterogeneity and connectivity for woody vegetation and grasslands (Fig. S7), respectively, (3) between horizontal and vertical forest heterogeneity (Fig. S12a), and (4) between horizontal and temporal heterogeneity for croplands and grasslands, respectively (Fig. S12b-d). To keep data consistent in each SEM, the same datasets were used for % land-cover and horizontal heterogeneity calculations within each SEM. For example, when calculating % forest, we used a land cover map for an SEM for LC (*% LC forest*; Fig. 3a) while using a dominant forest tree species map for an SEM for forests (*% forest*; Fig. 3c). SEMs could not capture all relationships due to the absence of certain components of landscape heterogeneity, such as the configurational heterogeneity of grasslands (see Section 2.2.).

SEMs were modelled using the R packages *lavaan*, and standardised parameter estimates (std. est.) were calculated for regressions and covariances and plotted using the R packages *semPlot*. Variables with skewed distributions were transformed by square-root or cube-root (see details in Table S3), and orthogonal quadratic terms of % land-cover and heterogeneity indices were added to account for nonlinear relationships (e.g., Fig. S4). Linear terms described the association direction between variables, i.e., positive or negative, and quadratic terms represented the bending shape of parabolic curves, i.e., concave up or down. All variables were Z-transformed before modelling.

Principal component analysis (PCA; R package *vegan*) explored relationships among multiple landscape heterogeneity components across land-cover types. It supports interpreting and visualising complex high-dimensional datasets by reducing dimensionality while preserving variations. Standardising variables to zero mean and unit standard deviation was performed during PCA.

3. Results

3.1. Compositional and configurational heterogeneities

Spearman's correlation and Structural Equation Modeling (SEM) analyses revealed positive correlations between *H'* and *ED* both across LC and within individual land-cover types. The association level in SEM here means partial correlation after controlling for % land-cover and abiotic factors on *H'* and *ED* and accounting for the indirect effects along a compound path (see Fig. S5 and Table S2 for the full variables). *LC H'* and *LC ED* showed a strong correlation (rho = 0.73; Fig. 3b) and a substantial SEM association (std. est. = 0.64; Fig. 3a). Notably, the correlation between *LC H'* and *LC ED* varied with *% LC croplands*, ranging from 0.50 to 0.82 (Fig. 3b). Given that *% LC croplands* had the most substantial impact on LC heterogeneities among the three land-cover types (Fig. 3a), we analysed correlations per decile of *% LC croplands*. The *% LC croplands* was associated with *LC ED* by –0.52 and –0.26 of std. est. for the 1st and 2nd factors, respectively, and with *LC H'* by –0.38 and –0.46 with the 1st and 2nd factors, respectively (Fig. 3a; Fig. S6b; Fig. S6e). However, a strong negative correlation between *% LC forests* and *% LC croplands* was found (std. est. = –0.73), indicating a potential trade-off between forests and croplands across land-cover compositional gradients (Fig. 3a). Thus, we additionally examined decile correlations between *LC H'* and *LC ED* for *% LC forests*, ranging from rho = 0.45 to 0.72 (Fig. S16). Despite collinearity induced by the high mutual correlation of % land-cover with both *LC H'* and *LC ED*, the partial correlation between *LC H'* and *LC ED* remained strong in both decile correlations.

Focussing on forests, a weak correlation between *Tree H'* and *Tree ED* was observed (*rho* = 0.17; Fig. 3d), but SEM revealed a high partial correlation (std. est. = 0.79; Fig. 3c). Analysing landscapes with similar % forest at ten-percentile intervals, *Tree H'* and *Tree ED* correlations ranged from *rho* = 0.39 to 0.93, higher than the overall grid correlation (Fig. 3d). It corresponded with a larger SEM partial correlation than bivariate correlation between *Tree H'* and *Tree ED*. In croplands, a moderate correlation between *crop H'* and *crop ED* was found (*rho* = 0.52; Fig. 3f), but SEM indicated a low partial correlation (std. est. = 0.25; Fig. 3e). Contrary to forests, correlations between *crop H'* and *crop ED* per decile of % croplands were low (rho = 0.03 to 0.39) and disappeared in landscapes with minimal % cropland (Fig. 3f). It corresponded with the finding that the partial correlation between *crop H'* and *crop ED* was relatively low in SEM. This suggests that the moderate overall correlation between *crop H'* and *ED* is likely driven by strong positive effects of *% croplands* on both indices rather than a direct association. Thus, partial correlations between H' and ED were significant in forests but weak in croplands when accounting for % land-cover effects.

SEM analyses revealed opposite effects of *% forests* on *Tree H'* and *Tree ED*—one negative and one positive (Fig. 3c)—while *% croplands* had positive effects on both *crop H'* and *ED* (Fig. 3e). Correlation tests for deciles of % land-cover provided additional information about these relationships. In landscapes with minimal forests (e.g., <5%), diverse dominant tree species (high *Tree H'*) were present, indicating that forest diversity is relatively independent of *% forest*, with a slight negative association (Fig. 3c). Conversely, *Tree ED* was limited in less forested landscapes, showing significant restriction for % *forest* (see red dots and line in Fig. 3d). In extensively forested landscapes (e.g., >75%), both *Tree H'* and *Tree ED* varied widely and were highly correlated (*rho* = 0.93; see blue dots and line in Fig. 3d). Some large forests were dominated by a single species (e.g., spruce or beech), resulting in very low *H'* and *ED* (see an example in Fig. S14a).

In croplands, increases in *% croplands* corresponded with increases in *crop H'* and *ED*. Landscapes with low *% croplands* had low values for both indices, while those with high *% croplands* exhibited high values for both. Thus, a strong correlation of *% croplands* with both *crop H'* and *ED* induced superficial collinearity between these indices, even though their pure correlation was low. In extensively cropped landscapes, multiple crop types (high *crop H'*) with regular patch shapes and sizes were common, inducing less variance in *crop ED* (see an example in Fig. S14b). Similar patterns were observed in the quantile correlation between *H'* and *mean patch size,* another classical configurational heterogeneity index (Fig. S15).

3.2. Heterogeneities and connectivity

Although connectivity is often assumed to increase with configurational heterogeneity, our results suggest a more nuanced relationship. While *ED* and *connectivity* exhibited a strong positive correlation in simple pairwise analyses, SEM revealed a weak or negative path coefficient (here, partial regression coefficient) after accounting for % land-cover effects. The connectivity of woody vegetation showed a high correlation with *forest ED* (*rho* = 0.74; Fig. S9). However, in SEM, where collinearity with % land-cover was controlled, this relationship weakened and even became slightly negative (std. est. = –0.09 and 0.02 for the 1st and 2nd factors, respectively; Fig. 4a, Fig. S8b). This suggested that the apparent positive correlation was largely driven by the co-variation of *% forest* with both *woody connectivity* and *forest ED* rather than a direct link. Indeed, SEM indicated that *% forest* had strong positive effects on both *woody connectivity* and *forest ED* (linear std. est.=1.07 and 0.76, respectively; Fig. 4a).

A similar pattern was observed for grasslands, where *grass connectivity* and *grass ED* were highly correlated (*rho* = 0.94; Fig. S11). However, SEM revealed a strong negative association between *grass connectivity* and *grass ED* after controlling for *% grasslands* (std. est. = –0.71 and 0.12 for the 1st and 2nd factors, respectively; Fig. 4b; Fig. S8f). The strong pairwise correlation stemmed from *% grassland* influencing both *grass connectivity* and *grass ED* (linear std. est. = 1.67 and 0.97; Fig. 4b). Quantile correlations supported this negative association, ranging from −0.08 to −0.5 for woody features and −0.12 to −0.54 for grasslands, except in extreme deciles (Fig. S17).

3.3. Horizontal, vertical, and temporal heterogeneities

Despite moderate correlations between multi-dimensional heterogeneities (*rho* = 0.33–0.64; Fig. S10, S11), SEM revealed weaker partial correlations when accounting for % land-cover and land management practice. The standard deviation (SD) of canopy height, a vertical heterogeneity measure, had a limited SEM association with horizontal heterogeneities. SEM path coefficients for *canopy height SD* with *Tree ED* were 0.28 (linear) and -0.36 (quadratic), while with *Tree H'*, they were 0.06 and 0 (Fig. 5a, S13b, S13c). Temporal heterogeneities also showed limited associations with horizontal heterogeneities in SEM, except for *horizontal* and *temporal crop H'* (std. est.=0.65 and 0.05 for the 1st and 2nd factors, respectively; Fig. 5b). The associations between *horizontal* and *temporal crop ED* (interannual change rate) and *horizontal* and *temporal grass SD* were weaker (std. est.=0.07 and –0.04 for the 1st and 2nd factors, respectively, for the former and std. est.=0.25 and 0.08 for the 1st and 2nd factors for the latter, respectively; Fig. 5c, 5d).

3.4. Heterogeneities between multiple land-covers

While heterogeneities within single land-cover types were predominantly positively correlated (e.g., *rho* = 0.59 for *horizontal* and *temporal crop H'*), certain forest-related heterogeneities showed negative correlations (Fig. 6a). Between different land-cover types, correlations varied from negative (e.g., *rho* = −0.48 for *crop ED* and *woody connectivity*) to positive (e.g., *rho* = 0.58 for *Tree ED* and *LC ED*). Grassland-related heterogeneities exhibited minimal correlations with other land-cover heterogeneities. In the PCA, the first two principal components (PCs) explained 47% of the variance in multiple dimensions, land-cover types, and attributes of heterogeneities (Table S4). The first principal component (PC1; 29% variance) was positively influenced by forest- and LC-related heterogeneities but negatively by crop heterogeneities (Fig. 6b, Table S5). The second principal component (PC2; 18% variance) primarily represented grassland-related heterogeneities (Fig. 6b).

4. Discussion

Landscape heterogeneity has been shown to enhance biodiversity, ecosystem services, and resilience (van Nes and Scheffer 2005; Stein et al. 2014; Le Provost et al. 2022). However, further studies are needed to explore the relationships among different components of landscape heterogeneity, including vertical and temporal heterogeneity, as new data become available. Such research will help refine the selection of heterogeneity indices, guide site stratification, and control for key covariates or interactions in ecological analyses. This study examined complex relationships among multiple land-cover types, attributes, and dimensions of landscape heterogeneity at the national scale in Germany. Our findings highlight a strong association between horizontal heterogeneities, a weaker link between horizontal, vertical, and temporal heterogeneities, a negative association between heterogeneity and connectivity, and distinct contributions of different land-cover types to overall landscape heterogeneity.

Structural equation modelling revealed the significant influence of % land-cover on landscape heterogeneity and the collinearity among heterogeneity indices, emphasising the need to account for % land-cover effects when analysing landscape heterogeneity relationships.

4.1. Compositional and configurational heterogeneities

Previous studies have acknowledged the interdependency between compositional and configurational heterogeneities, recommending stratified random sampling to minimise correlation biases (Fahrig et al. 2011; Pasher et al. 2013; Perović et al. 2015). Our findings further emphasise the necessity of controlling for % land-cover when designing stratification approaches to study ecological responses to heterogeneity. Without such controls, site selection may inadvertently favour landscapes with biased % land-cover distributions. For instance, landscapes with high edge density of all land-cover types (high *LC ED*) are more likely to have low shares of cropland (low *% LC croplands*) (Fig. 3a; Fig. S5a; Fig. S6b). We also found that the relationship between compositional (*H'*) and configurational heterogeneity (*ED*) varied between forests and croplands, likely due to the differing interactions of % land-cover with these heterogeneities. Forests exhibited a weak correlation but a significant partial correlation between *Tree H'* and *Tree ED* when controlling for *% forests*, whereas croplands displayed a moderate correlation but a weaker partial correlation in SEM when controlling for *% croplands*. These results at broad spatial scales suggest that failing to account for % land-cover can conceal collinearity, like in German forests, or exaggerate it, like in German croplands.

Configurational heterogeneity (often referred to as habitat fragmentation) and % land-cover should also be disentangled when assessing their effects on ecological responses (Fahrig 2017). While a meta-analysis on croplands found no intrinsic correlation between % land-cover and configurational heterogeneity (Martin et al. 2019), our study revealed a practical association in German forests and croplands at a national scale and 3 km landscape grain. This relationship may vary with spatial scale, necessitating further investigation across different extents and grain sizes (see comparison with 2-km landscape grain in Fig. S18).

Although pairwise correlations between compositional and configurational heterogeneities, as well as between % land-cover and configurational heterogeneity, have been assessed in previous studies, the broader correlation patterns involving % land-cover have rarely been explored. Our study provides new insights by demonstrating that the relationship between compositional and configurational heterogeneities is mediated by % land-cover, with distinct patterns observed across forests, croplands, and all land-cover types.

4.2. Heterogeneities and connectivity

Although connectivity is not strictly a form of heterogeneity, it is often assumed that increased configurational heterogeneity enhances functional connectivity, thereby benefiting biodiversity (Fahrig 2017). In a literature review, higher connectivity was the most frequently speculated reason for the positive effects of fragmentation on ecological responses (Fahrig 2017). Some studies have even used connectivity and configurational heterogeneity interchangeably (Estrada-Carmona et al. 2022; Tonetti et al. 2023). As expected, we found a positive correlation between edge density and connectivity in forests and grasslands (Fig. S9, Fig. S11). However, after controlling for % land-cover, the partial association between edge density and connectivity turned negative in SEM for woody features and grasslands, supported by quantile correlation analysis (Fig. S17). In landscapes with similar % land-cover, those with lower edge density exhibited higher connectivity (Fig. S19). This suggests that increasing configurational heterogeneity reduces connectivity by increasing fragmentation (i.e., patch isolation). Our study again underscores the importance of considering % land-cover when interpreting the relationship between configurational heterogeneity and connectivity, as their pure association may be negative rather than positive.

4.3. Horizontal, vertical, and temporal heterogeneities

The associations among multi-dimensional heterogeneities were generally weak but consistently positive. Since MacArthur and MacArthur (1961), the significance of vertical heterogeneity for biodiversity has been widely recognised, and advancements in remote sensing have even expanded research on 3-D structural complexity (Müller et al. 2010; Davies and Asner 2014; Seidel et al. 2020). However, the broader collinearity patterns between horizontal and vertical heterogeneity remain underexplored. Our findings suggest that vertical heterogeneity (*canopy height SD*) is largely independent of horizontal heterogeneities. Interestingly, SEM analysis revealed a negative relationship between *Tree H'* and *canopy height SD* with *% forest*, challenging the expectation that heterogeneity scales positively with the area (Stein et al. 2014). Our SEM analysis of forests might explain why a previous meta-analysis could not find positive effects of the area on plant diversity and vegetation complexity (Stein et al. 2014) (please see more discussion on *Tree H'* in session 4.1).

Temporal heterogeneity displayed diverse associations across land-cover types and attributes. In croplands, strong correlations between *horizontal* and *temporal H'* suggest that compositional heterogeneity in crop types is closely linked to interannual crop diversity. This implies that farmers who cultivate more diverse crops change crop types more frequently over the years. However, cultivation on small split fields (high *crop ED*) was not associated with frequent changes in crop type by year (high *temporal crop ED*) (Fig. 5c). Grasslands exhibited only weak correlations between horizontal and temporal heterogeneity. Variations in mowing frequency in landscapes within a single year were only lightly associated with temporal variations in mowing frequency across years. While temporal heterogeneity is increasingly recognised as a key factor influencing biodiversity (Vasseur et al. 2013), its effects remain inconsistent across studies. Some studies found positive effects of temporal variability of productivity, crop type, or management on biodiversity (Allan et al. 2014; Doležal et al. 2019;

Martínez-Núñez et al. 2022), while others found negative (Alavi and King 2020) or varied effects by functional groups (Coops et al. 2019; Beyer et al. 2021). Even though environmental conditions along the temporal dimension are determinant factors for the extinction rate of most populations, temporal heterogeneity was barely explored due to the cost of frequent collection of species and land cover data. Using recently published crop type and mowing frequency maps across four years, we first checked the general correlation between conventional horizontal and interannual heterogeneity at a national extent, showing varied but mostly strong independence of vertical or temporal heterogeneities. These results underscore the importance of considering multi-dimensional heterogeneities in landscapes. Further investigation is needed to study how temporal heterogeneity can differ by grain scale, e.g., intra-annual or inter-annual scale, and how such difference can influence the association between multi-dimensional heterogeneity across land-covers and attributes.

4.4. Heterogeneities between multiple land-covers

Correlations and PCA among landscape heterogeneities of multiple dimensions, attributes, and land-covers revealed overarching patterns of landscape heterogeneity at a national scale. Positive correlations were predominant within single land-cover types, while heterogeneities across different land-covers were generally negatively correlated. Notably, cropland heterogeneities exhibited negative correlations with forest and LC heterogeneities, which were positively correlated.

PCA further underscored the unique contributions of forest-, crop-, and grassland-related heterogeneities to overall landscape heterogeneity. On a national scale, overall landscape heterogeneity is primarily driven by forest and LC heterogeneities, with cropland heterogeneities contributing negatively. This divergence likely reflects the influence of % land-cover—for instance, a decrease in % forest is often accompanied by an increase in % cropland

(Figs. 3a and S20a), inducing a decrease in forest heterogeneities and an increase in cropland heterogeneities. Thus, the trade-off between forests and croplands for land-cover likely shapes the divergence between forest and cropland heterogeneities. Meanwhile, LC heterogeneity showed a trend similar to that of forest heterogeneity, both decreasing with increasing cropland heterogeneity—likely driven by a rise in % cropland (see also Figs. 3a and 3e). In Germany, the conversion of forests to intensively managed croplands likely would lead to a reduction in overall landscape heterogeneity, particularly in configurational attributes, given the more regular shape of cropland patches (Figs. 3a, 3c; Fig. S14b). In contrast, grassland heterogeneities showed limited correlations with those of other land-cover types, emphasising their distinct contribution as captured by the second principal component.

4.5. Limitation

It is important to recognise that heterogeneity can be quantified in numerous ways—not only by land-cover type, attribute, and dimension but also by the specific equations, parameters, spatial resolutions, classification schemes, or temporal resolutions employed. Consequently, the choice of heterogeneity indices should be tailored to the objectives of each study, as no single universal index exists. Moreover, the observed associations among landscape heterogeneities may differ with alternative methodological choices, as well as with variations in land-use history, landform, and socio-economic factors that shape trade-offs among land-cover types. For instance, the average field size in German croplands differs from that in Korea or the USA (Fritz et al. 2015), suggesting that heterogeneity associations within and between croplands and other land-cover types could vary across countries. Studies across countries or administrative regions—likely differing in social context—are therefore needed to generalise these findings.

5. Conclusion

Overall, our study challenges classical assumptions about landscape heterogeneity. First, as % land-cover mediates correlations between compositional and configurational heterogeneities, controlling for its effects is crucial to avoid biased interpretations. In particular, our findings highlight the importance of accounting for % land-cover when designing stratification approaches to study ecological responses to landscape heterogeneity. Second, as % land-cover also mediates the relationship between configurational heterogeneity and connectivity, their presumed positive correlation should be reconsidered—calling into question their mixed interpretation without empirical testing. Third, the relative independence of vertical and temporal heterogeneities from horizontal heterogeneities opens new avenues for investigating how ecological responses vary along these additional dimensions. Lastly, landscape heterogeneity is shaped by interactions between land-cover types, with forests enhancing and croplands reducing configurational heterogeneity; however, heterogeneity patterns vary with index, regional context, and land-use history, highlighting the need for cross-national studies.

Author contributions

SB, AK, CW, CP, SS, PH, TK, and SH conceived the idea for the study, which was further developed through multiple discussions with all authors. SB performed the data analysis and wrote the first draft of the manuscript. AK, CW, MS, PH, TK, and SH contributed to refining the data analysis. All authors participated in revising the manuscript and approved the final version for publication.

References

1. Abrego N, Norros V, Halme P, et al (2018) Give me a sample of air and I will tell which species are found from your region: Molecular identification of fungi from airborne spore samples. Mol Ecol Resour 18:511–524. https://doi.org/10.1111/1755-0998.12755
2. Alavi N, King D (2020) Evaluating the Relationships of Inter-Annual Farmland Vegetation Dynamics with Biodiversity Using Multi-Spatial and Multi-Temporal Remote Sensing Data. Remote Sensing 12:1479. https://doi.org/10.3390/rs12091479
3. Allan E, Bossdorf O, Dormann CF, et al (2014) Interannual variation in land-use intensity enhances grassland multidiversity. Proc Natl Acad Sci USA 111:308–313. https://doi.org/10.1073/pnas.1312213111
4. Bae S, Levick SR, Heidrich L, et al (2019) Radar vision in the mapping of forest biodiversity from space. Nat Commun 10:4757. https://doi.org/10.1038/s41467-019-12737-x
5. Beyer N, Gabriel D, Westphal C (2021) Contrasting effects of past and present mass-flowering crop cultivation on bee pollinators shaping yield components in oilseed rape. Agriculture, Ecosystems & Environment 319:107537. https://doi.org/10.1016/j.agee.2021.107537
6. Blickensdörfer L, Oehmichen K, Pflugmacher D, et al (2024) National tree species mapping using Sentinel-1/2 time series and German National Forest Inventory data. Remote Sensing of Environment 304:114069. https://doi.org/10.1016/j.rse.2024.114069
7. Blickensdörfer L, Schwieder M, Pflugmacher D, et al (2022) Mapping of crop types and crop sequences with combined time series of Sentinel-1, Sentinel-2 and Landsat 8 data for Germany. Remote Sensing of Environment 269:112831. https://doi.org/10.1016/j.rse.2021.112831
8. Coops NC, Bolton DK, Hobi ML, Radeloff VC (2019) Untangling multiple species richness hypothesis globally using remote sensing habitat indices. Ecological Indicators 107:105567. https://doi.org/10.1016/j.ecolind.2019.105567
9. Davies AB, Asner GP (2014) Advances in animal ecology from 3D-LiDAR ecosystem mapping. Trends in Ecology & Evolution 29:681–691. https://doi.org/10.1016/j.tree.2014.10.005
10. Deutscher Wetterdienst (DWD) (2021) Daily grids of soil moisture under grass for Germany, Version v2.0
11. Doležal J, Lanta V, Mudrák O, Lepš J (2019) Seasonality promotes grassland diversity: Interactions with mowing, fertilisation and removal of dominant species. Journal of Ecology 107:203–215. https://doi.org/10.1111/1365-2745.13007
12. Estrada-Carmona N, Sánchez AC, Remans R, Jones SK (2022) Complex agricultural landscapes host more biodiversity than simple ones: A global meta-analysis. Proceedings of the National Academy of Sciences 119:e2203385119. https://doi.org/10.1073/pnas.2203385119
13. Fahrig L (2017) Ecological Responses to Habitat Fragmentation Per Se. Annual Review of Ecology, Evolution, and Systematics 48:1–23. https://doi.org/10.1146/annurev-ecolsys-110316-022612

14. Fahrig L, Baudry J, Brotons L, et al (2011) Functional landscape heterogeneity and animal biodiversity in agricultural landscapes. Ecology Letters 14:101–112. https://doi.org/10.1111/j.1461-0248.2010.01559.x

15. Federal Statistical Office and the statistical offices of the Länder (2020) Atlas Agrarstatistik

16. Fick SE, Hijmans RJ (2017) WorldClim 2: new 1-km spatial resolution climate surfaces for global land areas. International Journal of Climatology 37:4302–4315. https://doi.org/10.1002/joc.5086

17. Fijen TPM, Eeraerts M, Osterman J, et al (2025) Crop diversification for pollinator conservation. Landsc Ecol 40:19. https://doi.org/10.1007/s10980-024-02027-3

18. Fricke U, Steffan-Dewenter I, Zhang J, et al (2022) Landscape diversity and local temperature, but not climate, affect arthropod predation among habitat types. PLOS ONE 17:e0264881. https://doi.org/10.1371/journal.pone.0264881

19. Fritz S, See L, McCallum I, et al (2015) Mapping global cropland and field size. Global Change Biology 21:1980–1992. https://doi.org/10.1111/gcb.12838

20. Gámez-Virués S, Perović DJ, Gossner MM, et al (2015) Landscape simplification filters species traits and drives biotic homogenisation. Nat Commun 6:8568. https://doi.org/10.1038/ncomms9568

21. Grace JB, Keeley JE (2006) A Structural Equation Model Analysis Of Postfire Plant Diversity In California Shrublands. Ecological Applications 16:503–514. https://doi.org/10.1890/1051-0761(2006)016[0503:ASEMAO]2.0.CO;2

22. Heidrich L, Bae S, Levick S, et al (2020) Heterogeneity–diversity relationships differ between and within trophic levels in temperate forests. Nat Ecol Evol 4:1204–1212. https://doi.org/10.1038/s41559-020-1245-z

23. Hiederer R (2013) Mapping Soil Properties for Europe – Spatial Representation of Soil Database Attributes. Publications Office of the European Union, Luxembourg

24. Jung K, Kaiser S, Böhm S, et al (2012) Moving in three dimensions: effects of structural complexity on occurrence and activity of insectivorous bats in managed forest stands: *Bats and 3D forest structure*. Journal of Applied Ecology 49:523–531. https://doi.org/10.1111/j.1365-2664.2012.02116.x

25. Komonen A, Müller J (2018) Dispersal ecology of deadwood organisms and connectivity conservation. Conservation Biology 32:535–545. https://doi.org/10.1111/cobi.13087

26. Lang N, Jetz W, Schindler K, Wegner JD (2022) A high-resolution canopy height model of the Earth

27. Le Provost G, Schenk NV, Penone C, et al (2022) The supply of multiple ecosystem services requires biodiversity across spatial scales. Nat Ecol Evol 1–14. https://doi.org/10.1038/s41559-022-01918-5

28. MacArthur RH, MacArthur JW (1961) On Bird Species Diversity. Ecology 42:594–598. https://doi.org/10.2307/1932254

29. Martin EA, Dainese M, Clough Y, et al (2019) The interplay of landscape composition and configuration: new pathways to manage functional biodiversity and agroecosystem services across Europe. Ecology Letters 22:1083–1094. https://doi.org/10.1111/ele.13265

30. Martínez-Núñez C, Kleijn D, Ganuza C, et al (2022) Temporal and spatial heterogeneity of semi-natural habitat, but not crop diversity, is correlated with landscape pollinator richness. Journal of Applied Ecology 59:1258–1267. https://doi.org/10.1111/1365-2664.14137

31. Müller J, Stadler J, Brandl R (2010) Composition versus physiognomy of vegetation as predictors of bird assemblages: The role of lidar. Remote Sensing of Environment 114:490–495. https://doi.org/10.1016/j.rse.2009.10.006

32. NASA Shuttle Radar Topography Mission (SRTM) (2013) Shuttle Radar Topography Mission (SRTM) Global. Distributed by OpenTopography

33. Papanikolaou AD, Kühn I, Frenzel M, Schweiger O (2017) Landscape heterogeneity enhances stability of wild bee abundance under highly varying temperature, but not under highly varying precipitation. Landscape Ecol 32:581–593. https://doi.org/10.1007/s10980-016-0471-x

34. Pasher J, Mitchell SW, King DJ, et al (2013) Optimising landscape selection for estimating relative effects of landscape variables on ecological responses. Landscape Ecol 28:371–383. https://doi.org/10.1007/s10980-013-9852-6

35. Perović D, Gámez-Virués S, Börschig C, et al (2015) Configurational landscape heterogeneity shapes functional community composition of grassland butterflies. Journal of Applied Ecology 52:505–513. https://doi.org/10.1111/1365-2664.12394

36. Pflugmacher D, Rabe A, Peters M, Hostert P (2018) Pan-European land cover map of 2015 based on Landsat and LUCAS data. Supplement to: Pflugmacher, D et al. (2019): Mapping pan-European land cover using Landsat spectral-temporal metrics and the European LUCAS survey. Remote Sensing of Environment, 221, 583-595, https://doi.org/10.1016/j.rse.2018.12.001

37. Saura S, Estreguil C, Mouton C, Rodríguez-Freire M (2011) Network analysis to assess landscape connectivity trends: Application to European forests (1990–2000). Ecological Indicators 11:407–416. https://doi.org/10.1016/j.ecolind.2010.06.011

38. Schellhorn NA, Gagic V, Bommarco R (2015) Time will tell: resource continuity bolsters ecosystem services. Trends in Ecology & Evolution 30:524–530. https://doi.org/10.1016/j.tree.2015.06.007

39. Schwieder M, Wesemeyer M, Frantz D, et al (2022) Mapping grassland mowing events across Germany based on combined Sentinel-2 and Landsat 8 time series. Remote Sensing of Environment 269:112795. https://doi.org/10.1016/j.rse.2021.112795

40. Seibold S, Gossner MM, Simons NK, et al (2019) Arthropod decline in grasslands and forests is associated with landscape-level drivers. Nature 574:671–674. https://doi.org/10.1038/s41586-019-1684-3

41. Seidel D, Ammer C (2023) Towards a causal understanding of the relationship between structural complexity, productivity, and adaptability of forests based on principles of thermodynamics. Forest Ecology and Management 544:121238. https://doi.org/10.1016/j.foreco.2023.121238

42. Seidel D, Annighöfer P, Ehbrecht M, et al (2020) Deriving Stand Structural Complexity from Airborne Laser Scanning Data—What Does It Tell Us about a Forest? Remote Sensing 12:1854. https://doi.org/10.3390/rs12111854

43. Stein A, Gerstner K, Kreft H (2014) Environmental heterogeneity as a universal driver of species richness across taxa, biomes and spatial scales. Ecol Lett 17:866–880. https://doi.org/10.1111/ele.12277
44. Tonetti V, Pena JC, Scarpelli MD, et al (2023) Landscape heterogeneity: concepts, quantification, challenges and future perspectives. Environmental Conservation 50:83–92. https://doi.org/10.1017/S0376892923000097
45. Torresani M, Rocchini D, Alberti A, et al (2023) LiDAR GEDI derived tree canopy height heterogeneity reveals patterns of biodiversity in forest ecosystems. Ecological Informatics 76:102082. https://doi.org/10.1016/j.ecoinf.2023.102082
46. Torresani M, Rocchini D, Ceola G, et al (2024) Grassland vertical height heterogeneity predicts flower and bee diversity: an UAV photogrammetric approach. Sci Rep 14:809. https://doi.org/10.1038/s41598-023-50308-9
47. van Nes EH, Scheffer M (2005) Implications of Spatial Heterogeneity for Catastrophic Regime Shifts in Ecosystems. Ecology 86:1797–1807. https://doi.org/10.1890/04-0550
48. Vasseur C, Joannon A, Aviron S, et al (2013) The cropping systems mosaic: How does the hidden heterogeneity of agricultural landscapes drive arthropod populations? Agriculture, Ecosystems & Environment 166:3–14. https://doi.org/10.1016/j.agee.2012.08.013
49. Westphal C, Steffan-Dewenter I, Tscharntke T (2006) Bumblebees experience landscapes at different spatial scales: possible implications for coexistence. Oecologia 149:289–300. https://doi.org/10.1007/s00442-006-0448-6
50. Zhang Y, Haan NL, Landis DA (2020) Landscape composition and configuration have scale-dependent effects on agricultural pest suppression. Agriculture, Ecosystems & Environment 302:107085. https://doi.org/10.1016/j.agee.2020.107085

Figure legends

Figure 1. Components of landscape heterogeneity.

Figure 2 Workflow for calculating metrics from publicly available GIS data and conducting statistical analyses.

Figure 3. Relationship between *Shannon* diversity (*H'*) and edge density (ED) of land-covers, forests, and croplands.

Figure 4. SEMS for the relationship between ED and connectivity of (a) forests and small woody features in croplands and (b) grasslands.

Figure 5. SEMS for the relationship between (a) horizontal *H'* and ED and vertical standard deviation (SD) in forests, (b) between horizontal and temporal *H'* and (c) between horizontal and temporal ED in croplands, and (d) horizontal and temporal SD in grasslands.

Figure 6. Association between heterogeneity of multiple land-covers analysed by (a) *Spearman's* correlation and (b) principal component analysis.

Figure 7. Summary of association (partial regression in SEM) between heterogeneities of multiple attributes, dimensions, and land-covers.

Figures

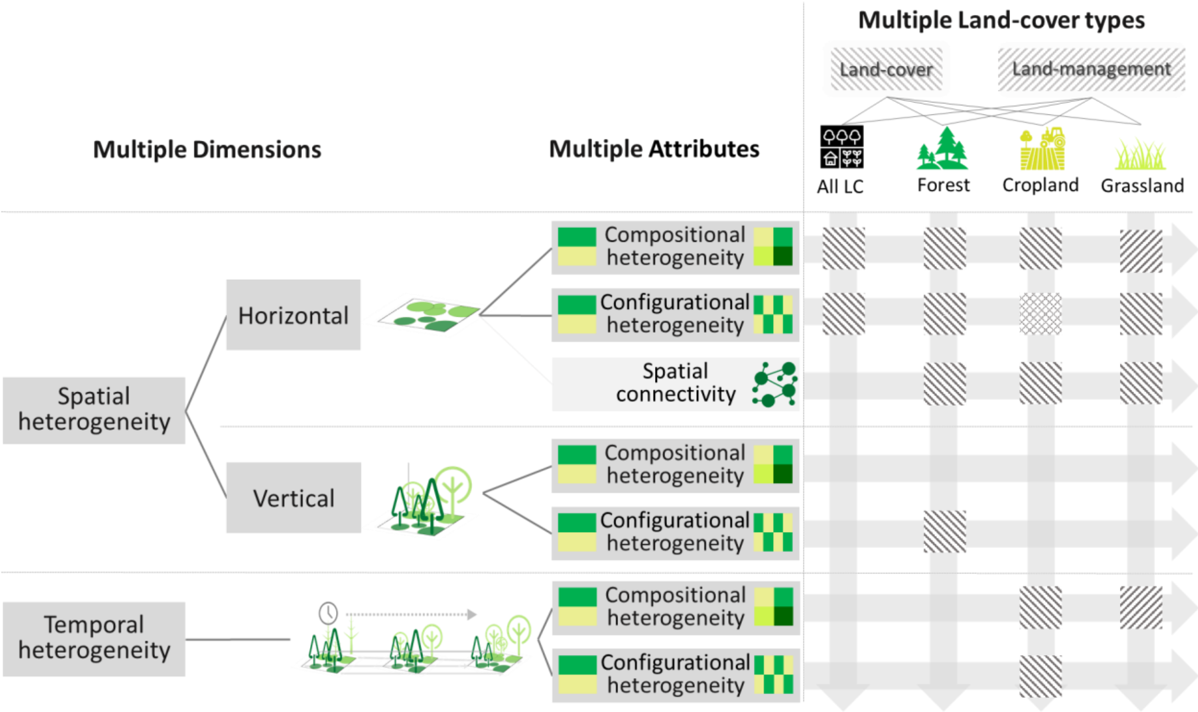

Figure 1. Components of landscape heterogeneity.

Landscape heterogeneity is characterised across three dimensions—horizontal, vertical, and temporal—based on two core attributes—compositional and configurational heterogeneity, along with spatial connectivity. These components can be quantified using land-cover types and land management practices, both across all land-cover types (hereafter LC) and within individual land-cover types, specifically forests, croplands, and grasslands. Although connectivity is not a form of heterogeneity, it is closely related and, therefore, included in the framework, indicated with a lighter colour. Heterogeneity components employed in this study are highlighted at their corresponding positions using the following visual indicators: falling diagonal lines for land-cover-based indices, rising diagonal lines for land management-based indices (applied only to grasslands), and intersecting falling and rising diagonals for metrics incorporating both (applied only to croplands).

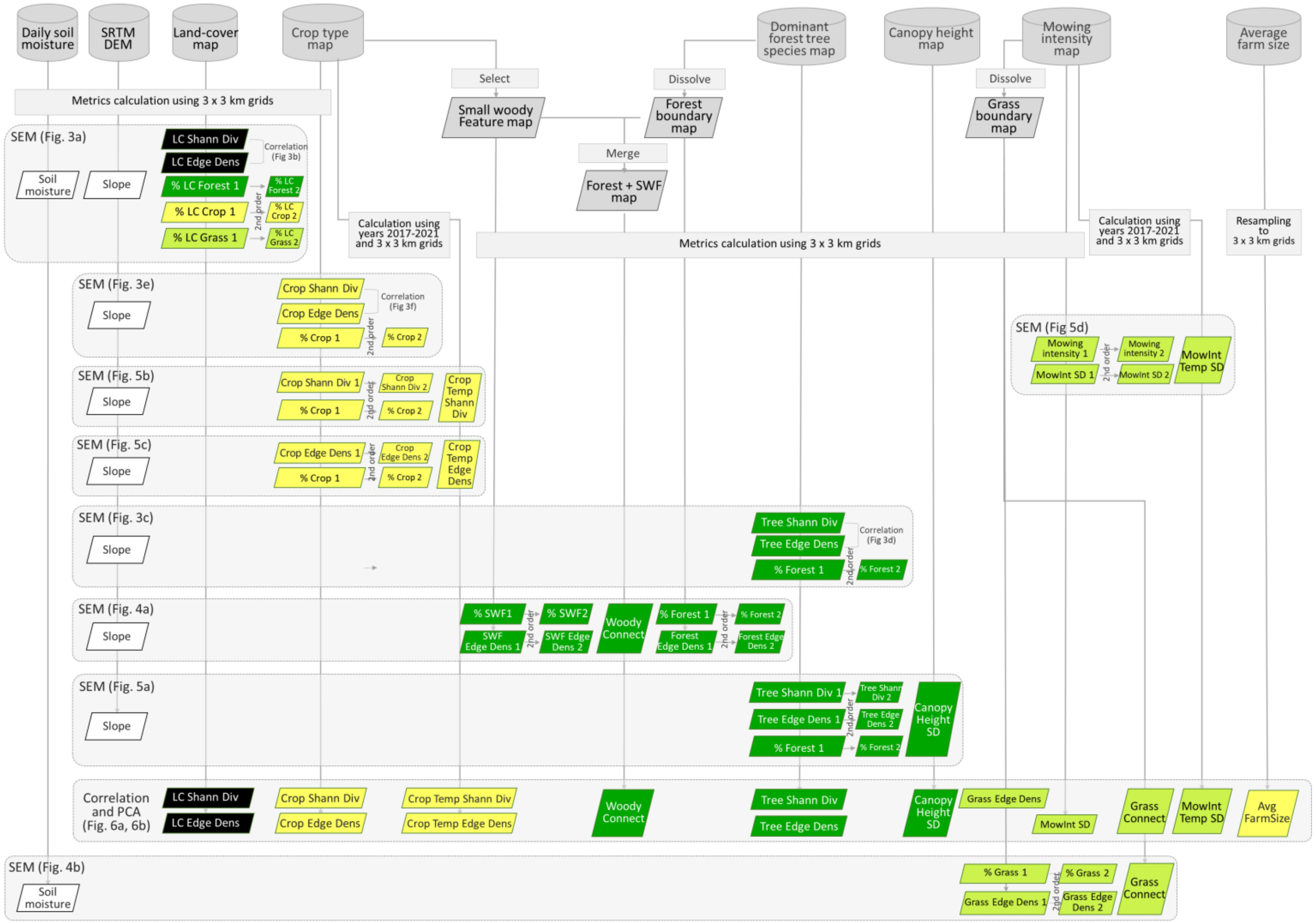

Figure 2 Workflow for calculating metrics from publicly available GIS data and conducting statistical analyses.

Descriptions of all metrics are provided in Table 1. SEM = Structural Equation Modeling; PCA = Principal Component Analysis.

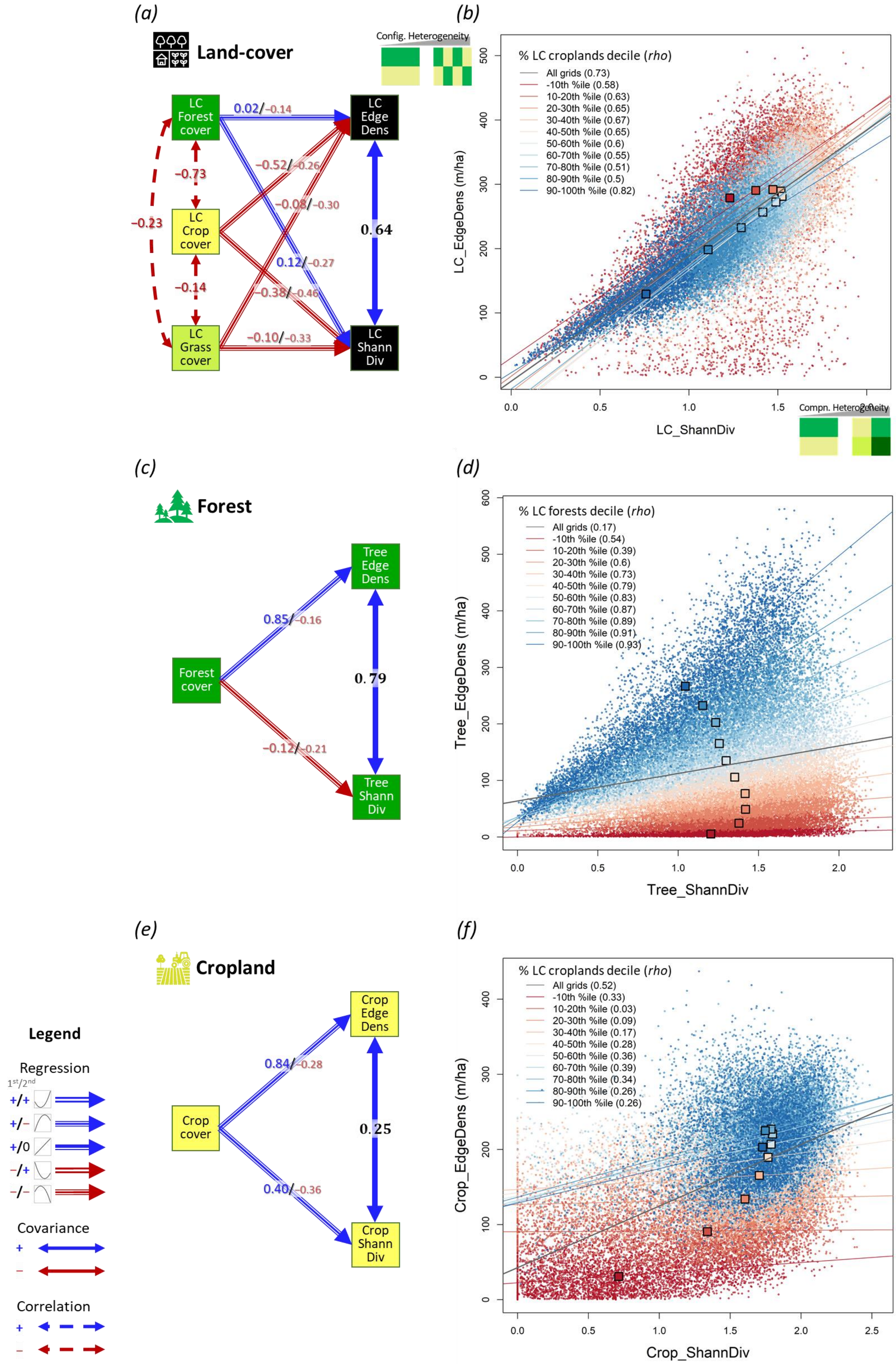
(a)
Land-cover
Config. Heterogeneity
LC Forest cover
LC Crop cover
LC Grass cover
LC Edge Dens
LC Shann Div
0.02/−0.14
−0.52/−0.26
−0.08/−0.30
0.12/−0.27
−0.38/−0.46
−0.10/−0.33
−0.73
−0.14
−0.23
0.64
(b)
% LC croplands decile (rho)
All grids (0.73)
-10th %ile (0.58)
10-20th %ile (0.63)
20-30th %ile (0.65)
30-40th %ile (0.67)
40-50th %ile (0.65)
50-60th %ile (0.6)
60-70th %ile (0.55)
70-80th %ile (0.51)
80-90th %ile (0.5)
90-100th %ile (0.82)
LC_EdgeDens (m/ha)
LC_ShannDiv
Compn. Heterogeneity
(c)
Forest
Forest cover
Tree Edge Dens
Tree Shann Div
0.85/−0.16
−0.12/−0.21
0.79
(d)
% LC forests decile (rho)
All grids (0.17)
-10th %ile (0.54)
10-20th %ile (0.39)
20-30th %ile (0.6)
30-40th %ile (0.73)
40-50th %ile (0.79)
50-60th %ile (0.83)
60-70th %ile (0.87)
70-80th %ile (0.89)
80-90th %ile (0.91)
90-100th %ile (0.93)
Tree_EdgeDens (m/ha)
Tree_ShannDiv
(e)
Cropland
Crop cover
Crop Edge Dens
Crop Shann Div
0.84/−0.28
0.40/−0.36
0.25
(f)
% LC croplands decile (rho)
All grids (0.52)
-10th %ile (0.33)
10-20th %ile (0.03)
20-30th %ile (0.09)
30-40th %ile (0.17)
40-50th %ile (0.28)
50-60th %ile (0.36)
60-70th %ile (0.39)
70-80th %ile (0.34)
80-90th %ile (0.26)
90-100th %ile (0.26)
Crop_EdgeDens (m/ha)
Crop_ShannDiv
Legend
Regression
1st/2nd
+/+
+/−
+/0
−/+
−/−
Covariance
+
−
Correlation
+
−

Figure 3. Relationship between *Shannon* diversity (*H'*) and edge density (ED) of land-covers, forests, and croplands.

Structural equation modellings (SEMs) for the relationship between *H'* and *ED* of (a) all land-cover types, (c) dominant tree species in forests, and (e) crop types. In SEM, unidirectional arrows represent regressions, while bidirectional solid arrows covariances and dashed arrows correlation. Only significant relationships were denoted as arrows with standardised parameter estimates (std. est.). On the arrows of regressions, the std. est. of first- and second-order factors (1^{st} and 2^{nd}), in order, were denoted. Blue arrows and numbers denoted positive relationships, and red arrows and numbers denoted negative ones for regressions, covariances, and correlation. For regressions, if the arrow included two relationships of the 1^{st}- and 2^{nd}-order factors, the colour of the arrows followed the signs (+ or –) of the 1^{st}-order factor, meaning positive or negative relationship, and the shape of arrows differs by the signs of the 2^{nd}-order factor, meaning hump-shaped or U-shaped curve. Full SEM relationships can be found in Fig. S5, and the relationship of each partial regression in Fig. S6. *Spearman*'s correlation between *H'* and *ED* (b) of all land-cover types, (d) of forests, (f) of croplands by deciles of coverage. Points from the red to blue spectrum indicate each 10^{th} decile of 3×3 km^2 grid cells from 0–10^{th} decile to 90^{th} –100^{th} decile and lines linear regression lines per decile. Squares represent median values of *H'* and *ED* per decile with corresponding colours. Each *Spearman*'s *rho* is written in the bracket of the legend. The % land-cover ranges of grids for each decile can be found in Table S6a.

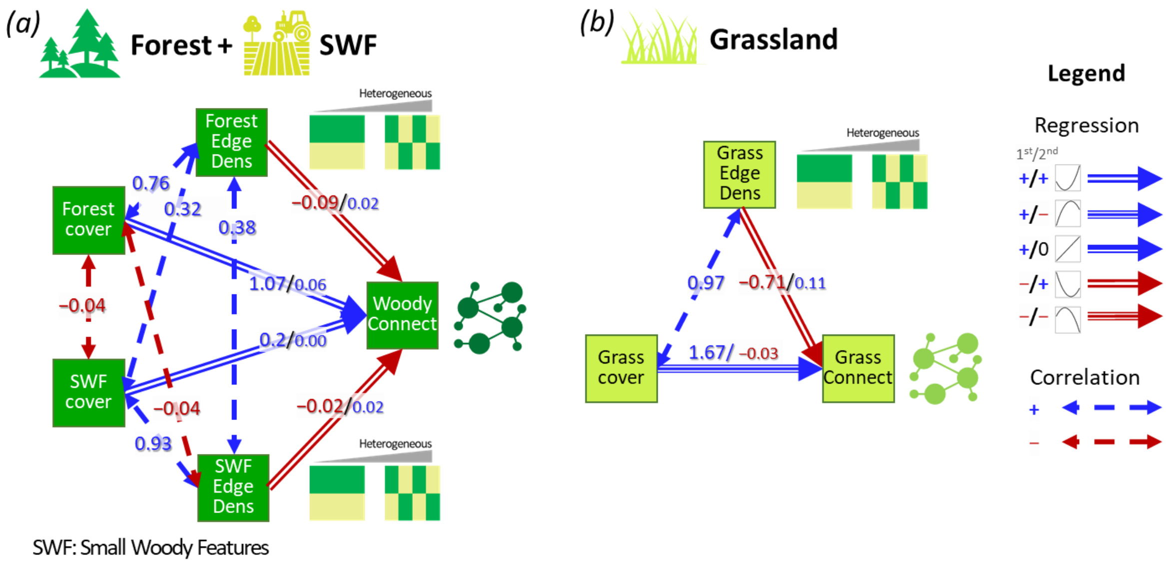

Figure 4. SEMS for the relationship between ED and connectivity of (a) forests and small woody features in croplands and (b) grasslands.

Full SEM relationships can be found in Fig. S10 and the relationship of each partial regression in Fig. S11.

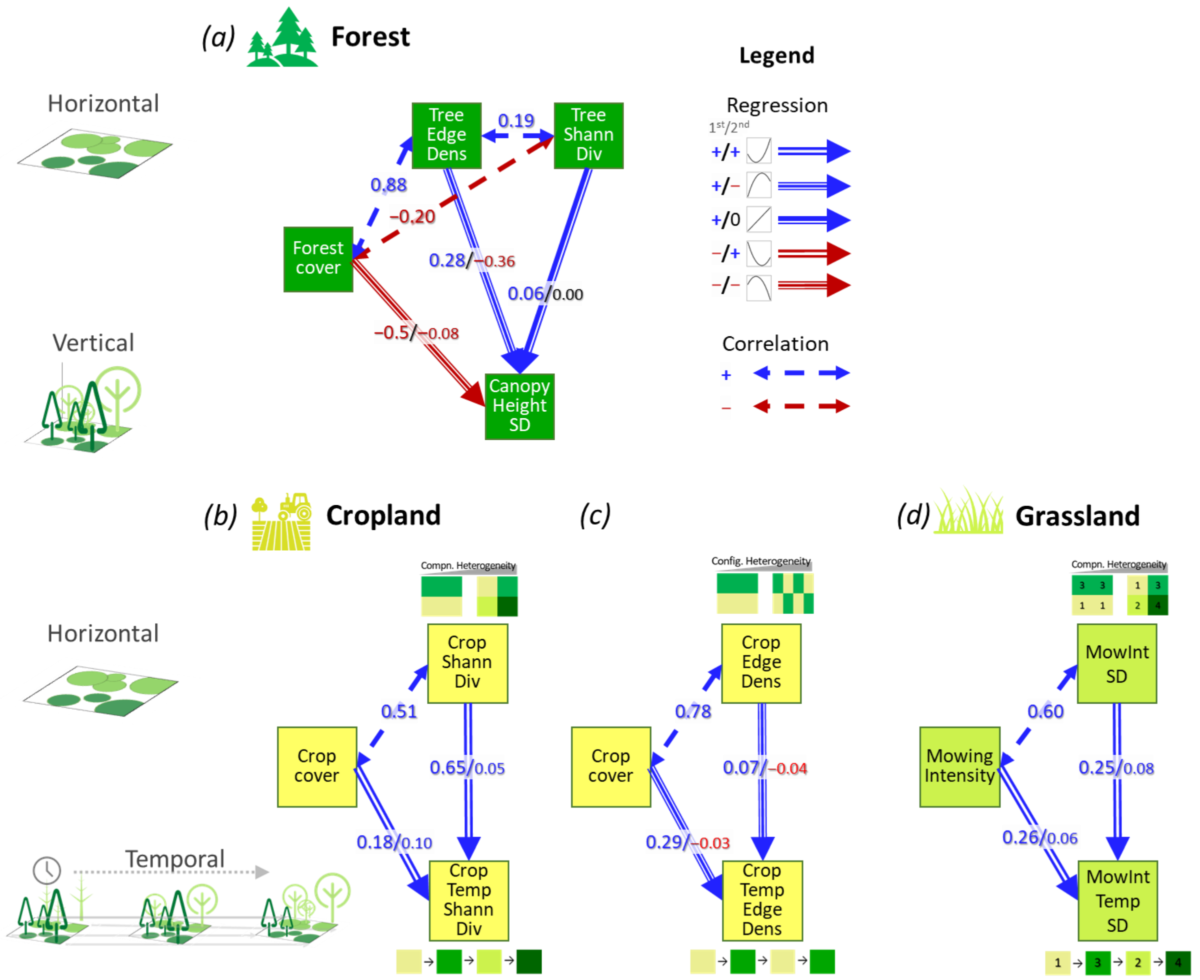

Figure 5. SEMS for the relationship between (a) horizontal *H'* and ED and vertical standard deviation (SD) in forests, (b) between horizontal and temporal *H'* and (c) between horizontal and temporal ED in croplands, and (d) horizontal and temporal SD in grasslands.

Full SEM relationships can be found in Fig. S12 and the relationship of each partial regression in Fig. S13.

(a)

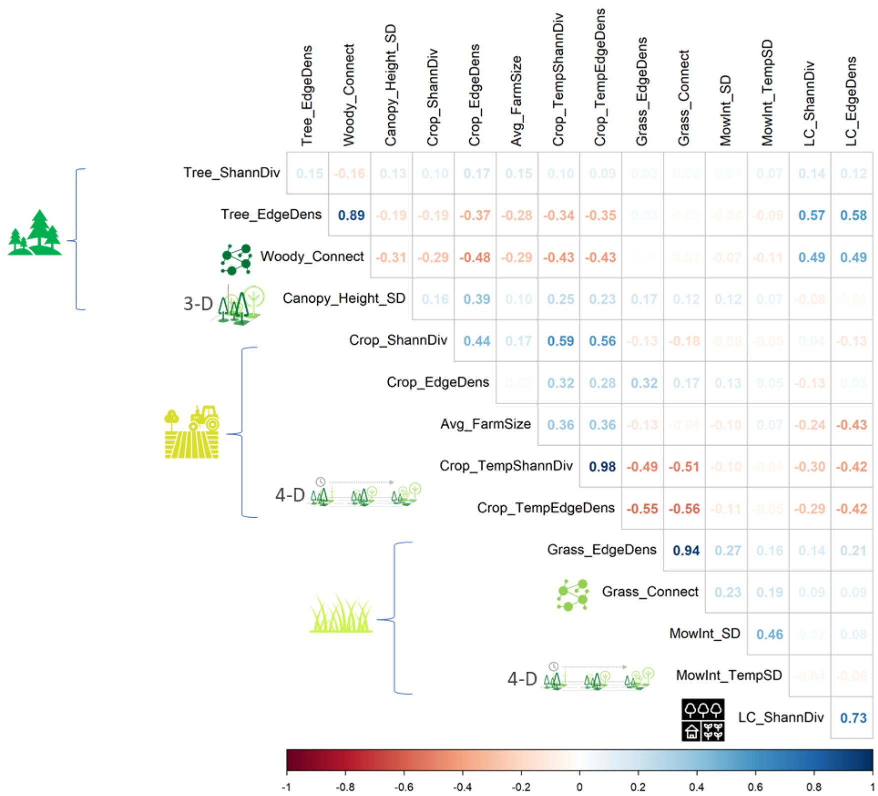
Tree_EdgeDens
Woody_Connect
Canopy_Height_SD
Crop_ShannDiv
Crop_EdgeDens
Avg_FarmSize
Crop_TempShannDiv
Crop_TempEdgeDens
Grass_EdgeDens
Grass_Connect
MowInt_SD
MowInt_TempSD
LC_ShannDiv
LC_EdgeDens
Tree_ShannDiv
3-D
4-D
4-D
-1
-0.8
-0.6
-0.4
-0.2
0
0.2
0.4
0.6
0.8
1

(b)

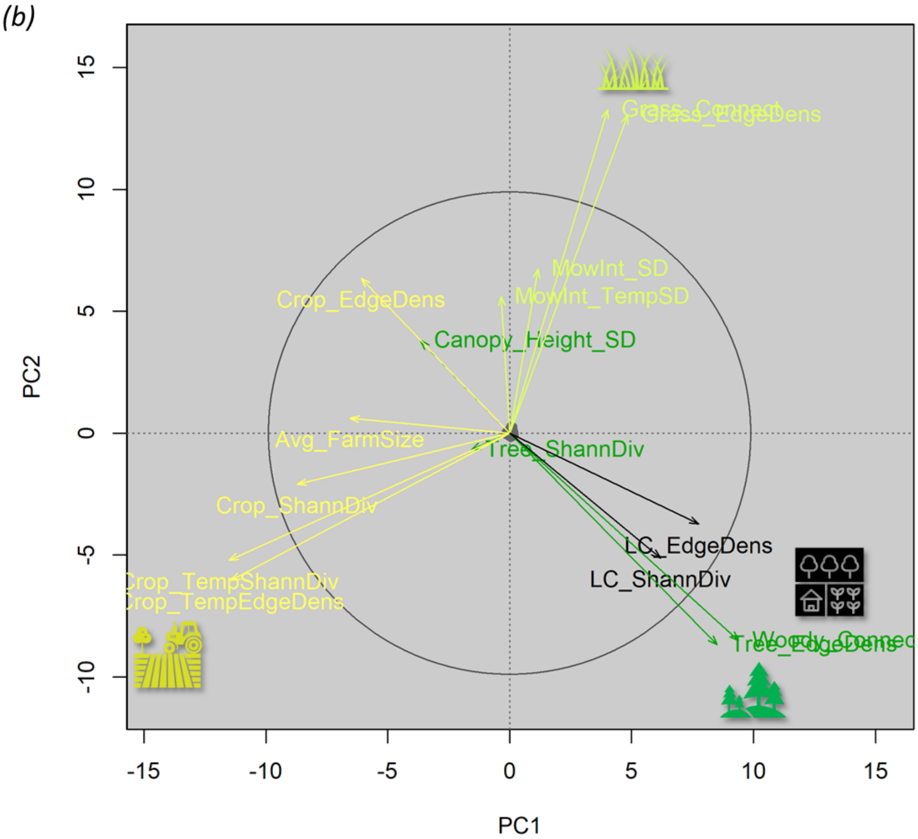
Grass_Connect
Grass_EdgeDens
MowInt_SD
MowInt_TempSD
Crop_EdgeDens
Canopy_Height_SD
Avg_FarmSize
Tree_ShannDiv
Crop_ShannDiv
Crop_TempShannDiv
Crop_TempEdgeDens
LC_EdgeDens
LC_ShannDiv
Woody_Connec
Tree_EdgeDens
PC1
PC2
-15
-10
-5
0
5
10
15

Figure 6. Association between heterogeneity of multiple land-covers analysed by (a) *Spearman*’s correlation and (b) principal component analysis.

(a) Positive correlations are displayed in blue, and negative ones in red. Colour intensity is proportional to the correlation coefficients. (b) PCA-biplot with the projected directionality and strength of the heterogeneity metrics on the first two principal components (PC1 and PC2). Green vectors represent forest-related, yellow crop-related, light-green grass-related, and black land-cover-related heterogeneity.

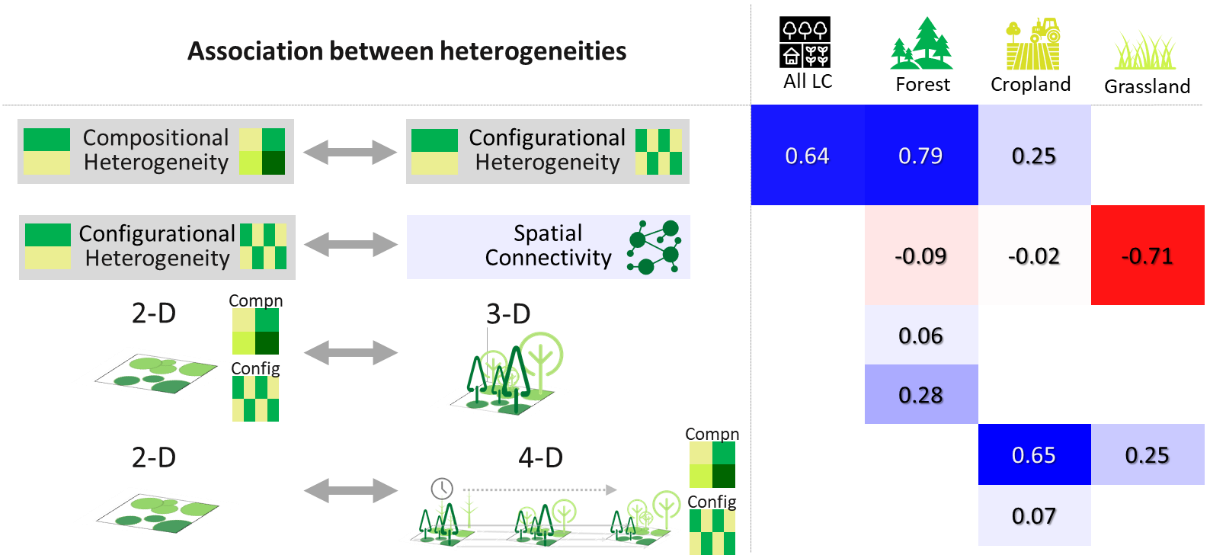

Figure 7. Summary of association (partial regression in SEM) between heterogeneities of multiple attributes, dimensions, and land-covers.

Blue colour denotes positive relationships, and red denotes negative ones. The colour brightness has been scaled based on the magnitude of the SEM standardised parameter estimates. If the relationship included two relationships of the first- and second-order factors, the colour and estimate followed the relationship of the first-order factor.

Table legends

Table 1. Indices of horizontal (2-D), vertical (3-D), and temporal heterogeneity in compositional (compn) and configurational (config) heterogeneities and spatial connectivity (connect) by land-cover types (LC) and land management practice (LM).

Tables

Table 1. Indices of horizontal (2-D), vertical (3-D), and temporal heterogeneity in compositional (compn) and configurational (config) heterogeneities and spatial connectivity (connect) by land-cover types (LC) and land management practice (LM).

H' denotes *Shannon* diversity, ED edge density, EC Equivalent Connectivity, SD standard deviation, and SWF small woody features.

Dimension			Land-cover	Attrib	Index name	Data	Year	Res.
Heterogeneity indices								
Spatial heterogeneity + connectivity	2-D	LC	Heterogeneity of all land-cover types	Compn	*LC H'*	Land cover map (Pflugmacher et al. 2018)	2015	30m
				Config	*LC ED*			
			Crop type heterogeneity	Compn	*Crop H'*	Crop type map (Blickensdörfer et al. 2022)	2020	30m
				Config	*Crop ED*			
			Dominant tree species heterogeneity	Compn	*Tree H'*	Dominant forest tree species map (Blickensdörfer et al. 2024)	2017, 2018	30m
				Config	*Tree ED*			
			Forest edge density	Config	*Forest ED*	Dominant forest tree species map	2017, 2018	30m
			SWF edge density	Config	*SWF ED*	Crop type map	2020	30m
			Grass edge density	Config	*Grass ED*	Mowing frequency map (Schwieder et al. 2022)	2020	30m
			Connectivity of woody vegetation	Connect	*Woody Connect*	SWF in crop type map + Forest map	2017, 2018	30m
			Grassland connectivity	Connect	*Grass Connect*	Mowing frequency map	2020	30m
		LM	Crop management heterogeneity	Config	*Avg FarmSize*	Average farm size on a 5 km grid (Federal Statistical Office and the statistical offices of the Länder 2020)	2020	5km
			Mowing frequency heterogeneity	Compn	*MowInt SD*	Mowing frequency map	2020	30m
	3-D	LC	Canopy height heterogeneity	Compn	*Canopy Height SD*	Canopy height model (Lang et al. 2022)	2020	30m
Temporal		LC	Crop temporal heterogeneity	Compn	*Crop Temp H'*	Crop type map	2017-2020	30m
				Config	*Crop Temp ED*			
		LM	Mowing frequency temporal heterogeneity	Compn	*MowInt Temp SD*	Mowing frequency map	2017-2020	30m
Non-heterogeneity indices								

Abiotic factors	Topography	Mean slope	*Slope*	SRTM DEM (NASA Shuttle Radar Topography Mission (SRTM) 2013)	2000	1 arc-second
	Soil	Mean soil moisture	*Soil moisture*	Daily soil moisture (Deutscher Wetterdienst (DWD) 2021)	1993-2022	1km
Spatial composition	LC	Proportion of forests in land cover map	*% LC Forest*	Land cover map	2015	30m
		Proportion of grasslands in land cover map	*% LC Grass*			
		Proportion of croplands in land cover map	*% LC Crop*			
		Proportion of forests in dominant forest tree species map	*% Forest*	Dominant forest tree species map	2017, 2018	30m
		Proportion of forests in crop type map	*% Crop*	Crop type map	2020	30m
		Proportion of SWF in crop type map	*% SWF*	Crop type map	2020	30m
		Proportion of grasslands in mowing frequency map	*% Grass*	Mowing frequency map	2020	30m
	LM	Mean mowing frequency	*Mowing intensity*	Mowing frequency map	2020	30m

Supplementary legends

Supplementary figures

Figure S1. Pie chart of main land-cover types in Germany based on land cover map (Pflugmacher et al. 2018).

Figure S2. Calculation of temporal heterogeneity in compositional and configurational attributes

Figure S3. Process to calculate woody vegetation connectivity on each 3 x 3 km grid cell.

Figure S4. *Spearman*'s correlation between (a) land-cover *Shannon* diversity (*H'*) and coverage of forests, grasslands, and croplands and (b) land-cover edge density (*ED*) and coverage of forests, grasslands, and croplands.

Figure S5. Full structural equation modellings (SEMs) of Fig. 3 between *H'* and ED of (a) across all land-cover types, (b) forests, and (c) croplands.

Figure S6. Relationship of partial regressions between predictors and response variables of each SEM in Fig. 3.

Figure S7. Full SEMs of Fig. 4 for the relationship between ED and connectivity of (a) forests and small woody features and (b) grasslands.

Figure S8. Relationship of partial regressions between predictors and response variables of each SEM in Fig. 4.

Figure S9. *Spearman*'s correlation between coverage, *H'*, ED, connectivity, and standard deviation of canopy height in forests.

Figure S10. *Spearman*'s correlation between coverage, *H'*, ED, and temporal *H'*, temporal ED (interannual change rate) of crop types in croplands.

Figure S11. *Spearman*'s correlation between coverage, ED, connectivity, mean mowing frequency, *H'* and temporal *SD* of mowing frequency in grasslands.

Figure S12. Full SEMS of Fig. 5 for the relationship between (a) horizontal *H'* and ED and vertical standard deviation (SD) in forests, (b) between horizontal and temporal *H'* and (c) between horizontal and temporal ED in croplands, and (d) horizontal and temporal SD in grasslands.

Figure S13. Relationship of partial regressions between predictors and response variables of each SEM in Fig. 5.

Figure S14. Comparison between (a) dominant tree type map and (b) crop type map in grid cells with high % forests and % croplands, respectively.

Figure S15. *Spearman*'s correlation between *H'* and mean patch size by deciles of coverage of (a) forests and (b) cropland. The mean patch size was transformed by cube root.

Figure S16. *Spearman*'s correlation between *H'* and ED of land-cover by deciles of % forest.

Figure S17. *Spearman*'s correlation between ED and connectivity by deciles of coverage of (a) forests and small woody features and (b) grasslands.

Figure S18. *Spearman*'s correlation between between *H'* and *ED* of all land-cover type with 2-km landscape grain.

Figure S19. Association between ED and connectivity.

Figure S20. Partial correlation plots between % forests, % croplands, and % grasslands in SEM of Fig. 3.

Supplementary tables

Table S1. All abiotic factors before variable selection

Table S2. Parameter estimates for the structural equation models (SEMs) shown in Figures 3–5. Variables shown in grey indicate non-significant effects ($p \geq 0.05$).

Table S3. Description of variables in SEMs in Figures 3-5. All variables in SEMs are described with their labels in Figures 3-5, variable names in Table S1, and transformation due to skewness of data distribution.

Table S4. Importance of components of principal component analysis (PCA) to explore datasets of horizontal, vertical, and temporal landscape heterogeneity indices.

Table S5. Coordinates of the arrowheads of horizontal, vertical, and temporal landscape heterogeneity indices

Table S6. Coverage ranges (% land-cover) of 3 × 3 km grids for each decile for quantile correlation between H' and ED of (a) land-cover types, (b) forest, and (c) croplands

Supplementary notes

Note S1. Equations of *Shannon* diversity index (*H'*) and edge density (*ED*)

References

Supplementary figures

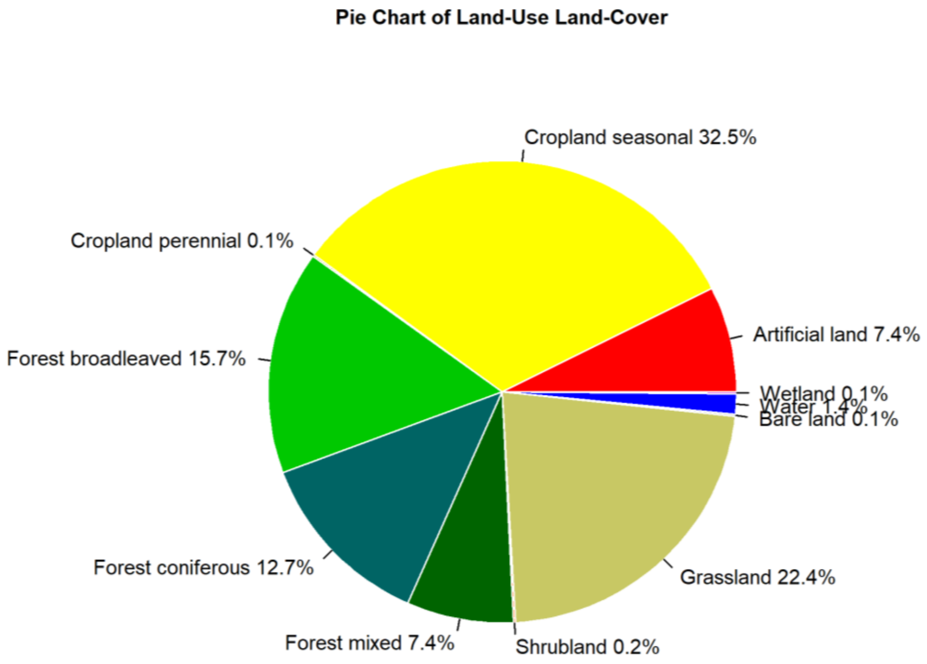

Figure S1. Pie chart of main land-cover types in Germany based on land cover map (Pflugmacher et al. 2018).

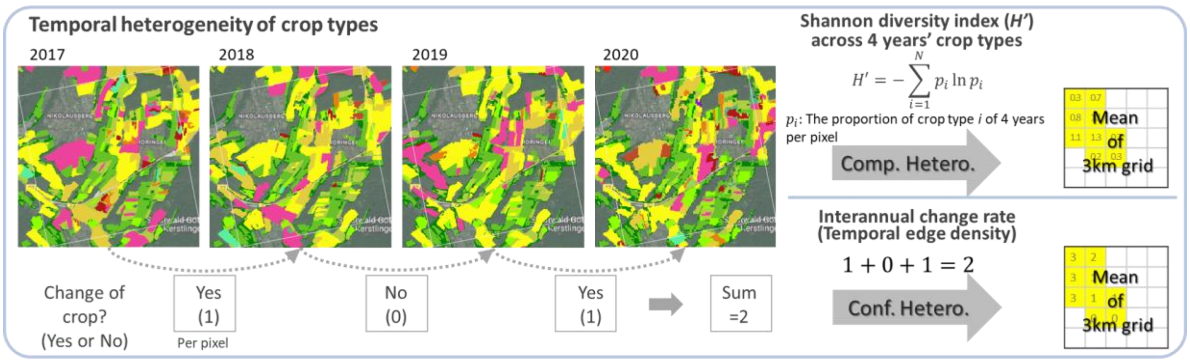

Figure S2. Calculation of temporal heterogeneity in compositional and configurational attributes

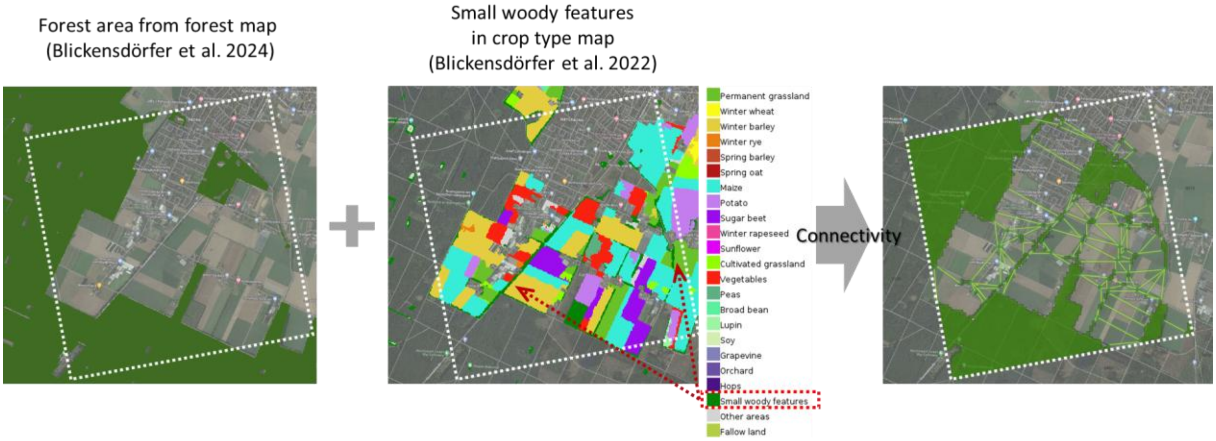

Figure S3. Process to calculate woody vegetation connectivity on each 3 x 3 km grid cell.

Woody vegetation connectivity was calculated by combining forest areas (Blickensdörfer et al. 2024) with small woody features derived from the crop type map (Blickensdörfer et al. 2022), treating them as habitat patches (dark green patches) for the connectivity index. Connectivity was calculated in each 3 x 3 km grid cell using *Graphab* (R package *graph4lg*). Least-cost paths between habitat patches (called a link set, denoted by light green lines) were generated using Euclidean distance and planar topology without a threshold distance. The planar link set, which limits connections to neighbouring patches identified by Voronoi polygons, serves as a reliable proxy for the complete link set. Connectivity was quantified using the Equivalent Connectivity metric, calculated as the square root of the summed product of patch areas weighted by interaction probability (Saura et al. 2011)

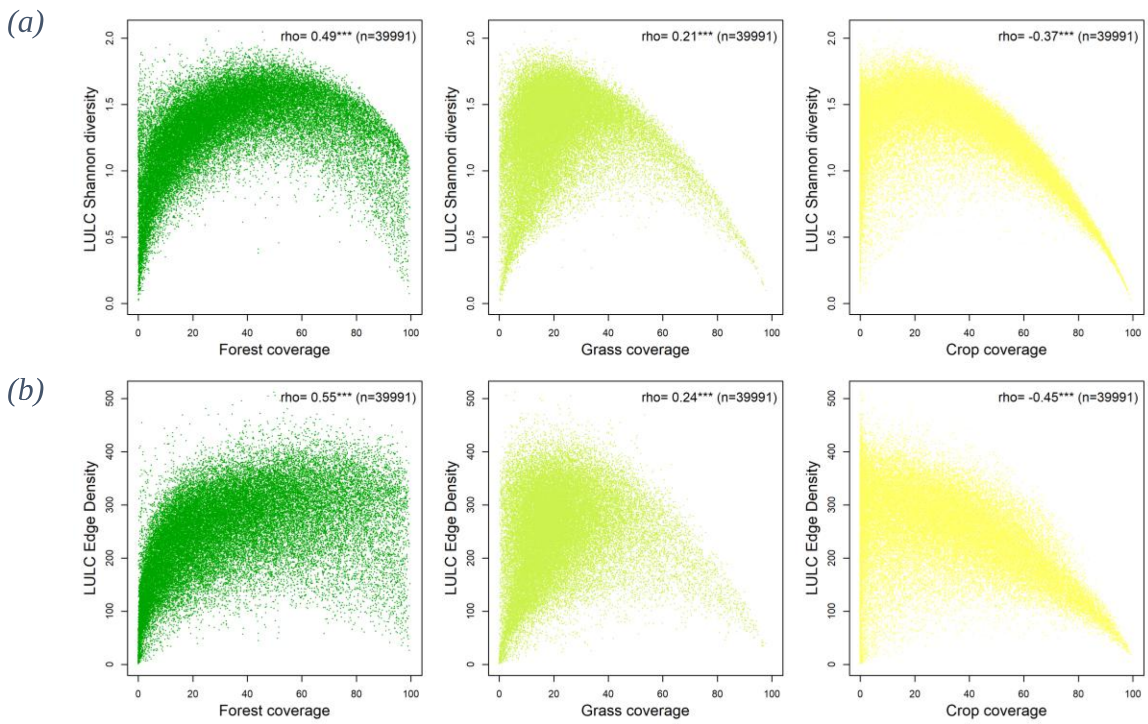

Figure S4. *Spearman*'s correlation between (a) land-cover *Shannon* diversity (*H'*) and coverage of forests, grasslands, and croplands and (b) land-cover edge density (*ED*) and coverage of forests, grasslands, and croplands.

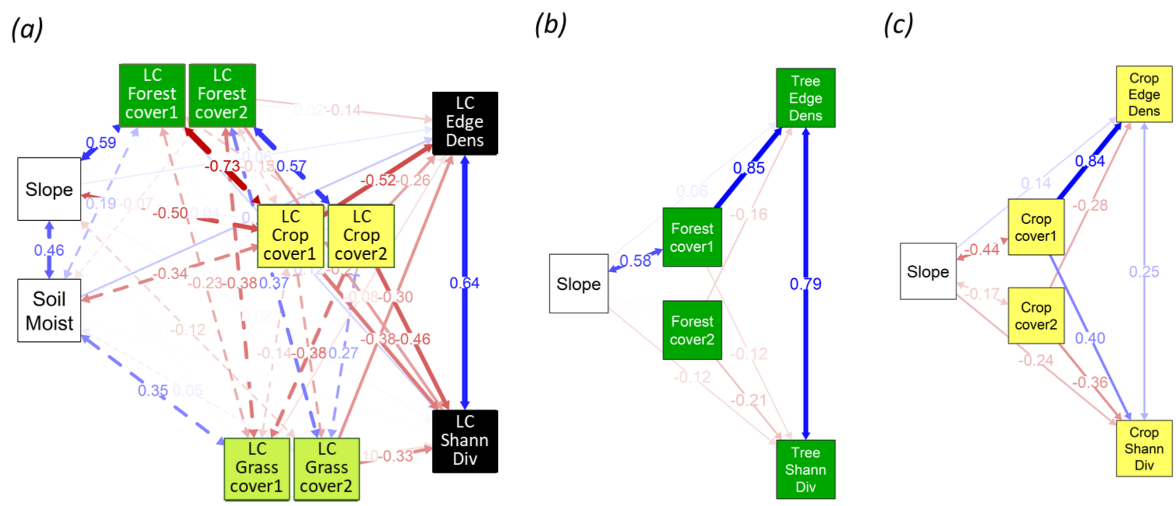

Figure S5. Full structural equation modellings (SEMs) of Fig. 3 between *H'* and ED of (a) across all land-cover types, (b) forests, and (c) croplands.

The simple version is shown in Fig. 3. In SEM, unidirectional arrows represent regressions, while bidirectional solid arrows covariances and dashed arrows correlation. Blue arrows denote positive relationships, and red arrows denote negative ones. The path thickness has been scaled based on the magnitude of the SEM standardised parameter estimates. Only significant relationships were denoted as arrows with standardised parameter estimates.

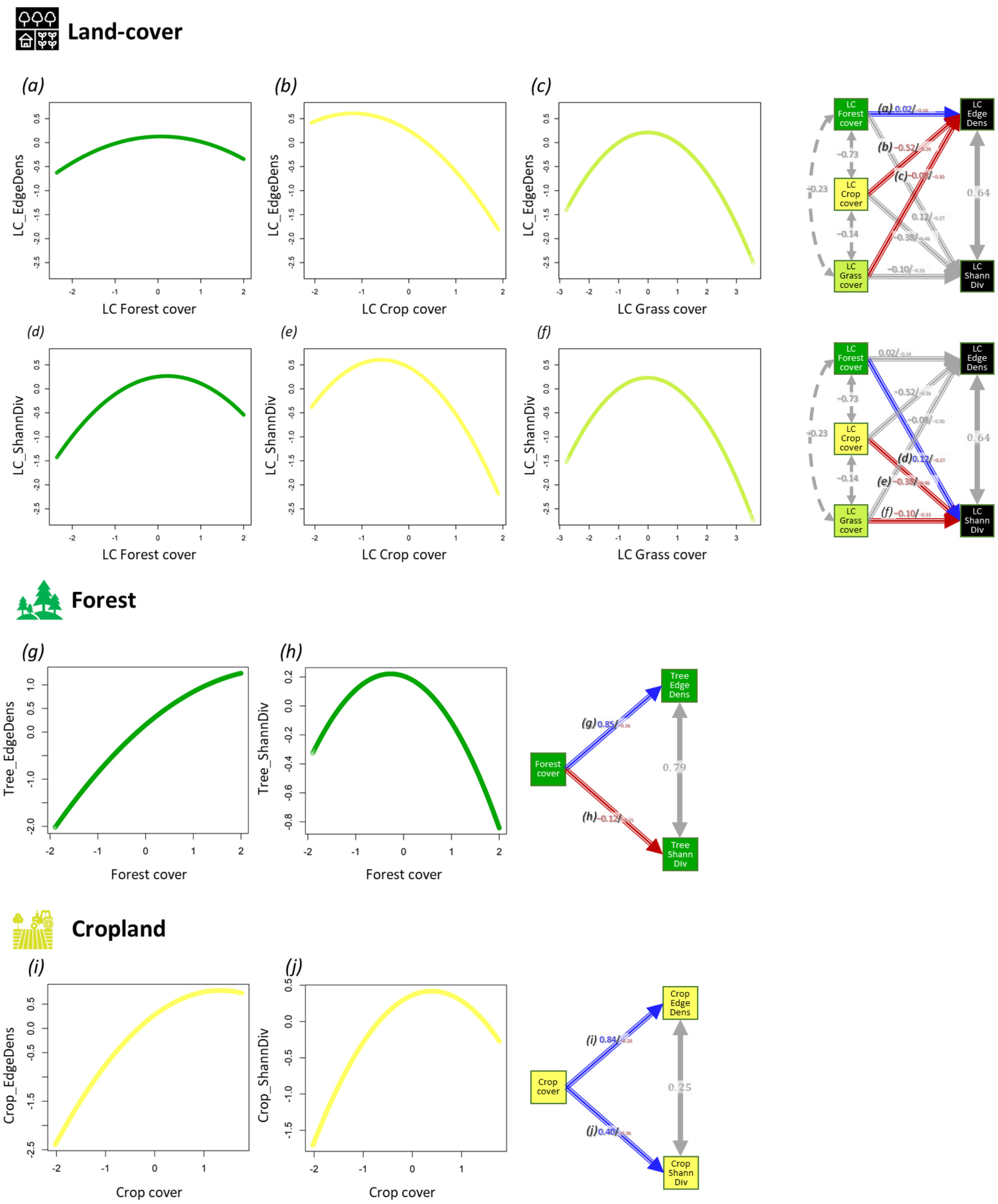

Figure S6. Relationship of partial regressions between predictors and response variables of each SEM in Fig. 3.

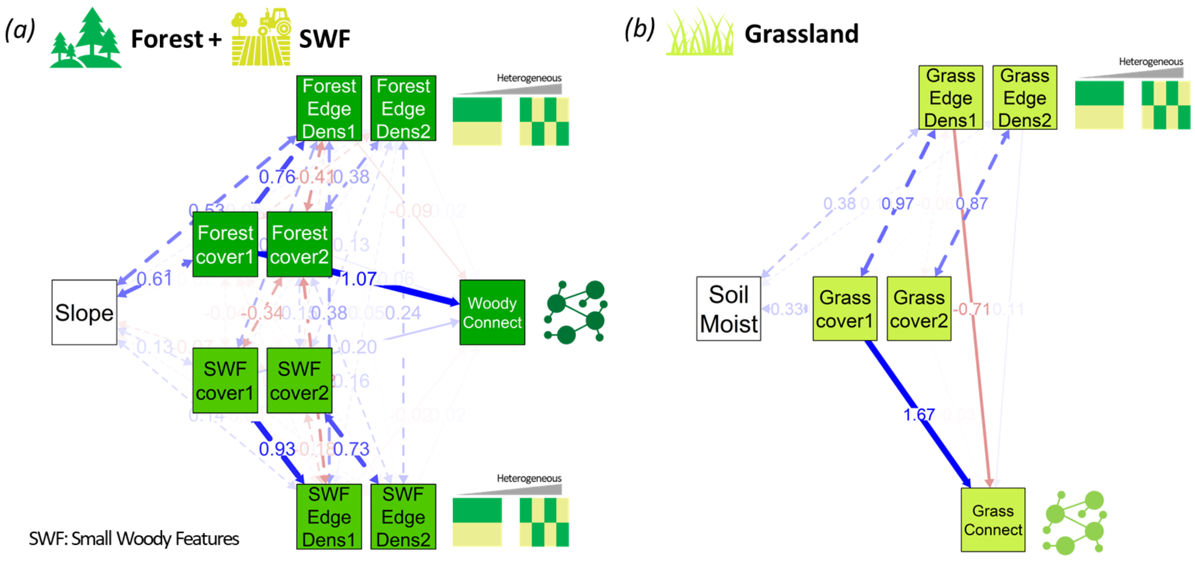

Figure S7. Full SEMs of Fig. 4 for the relationship between ED and connectivity of (a) forests and small woody features and (b) grasslands.

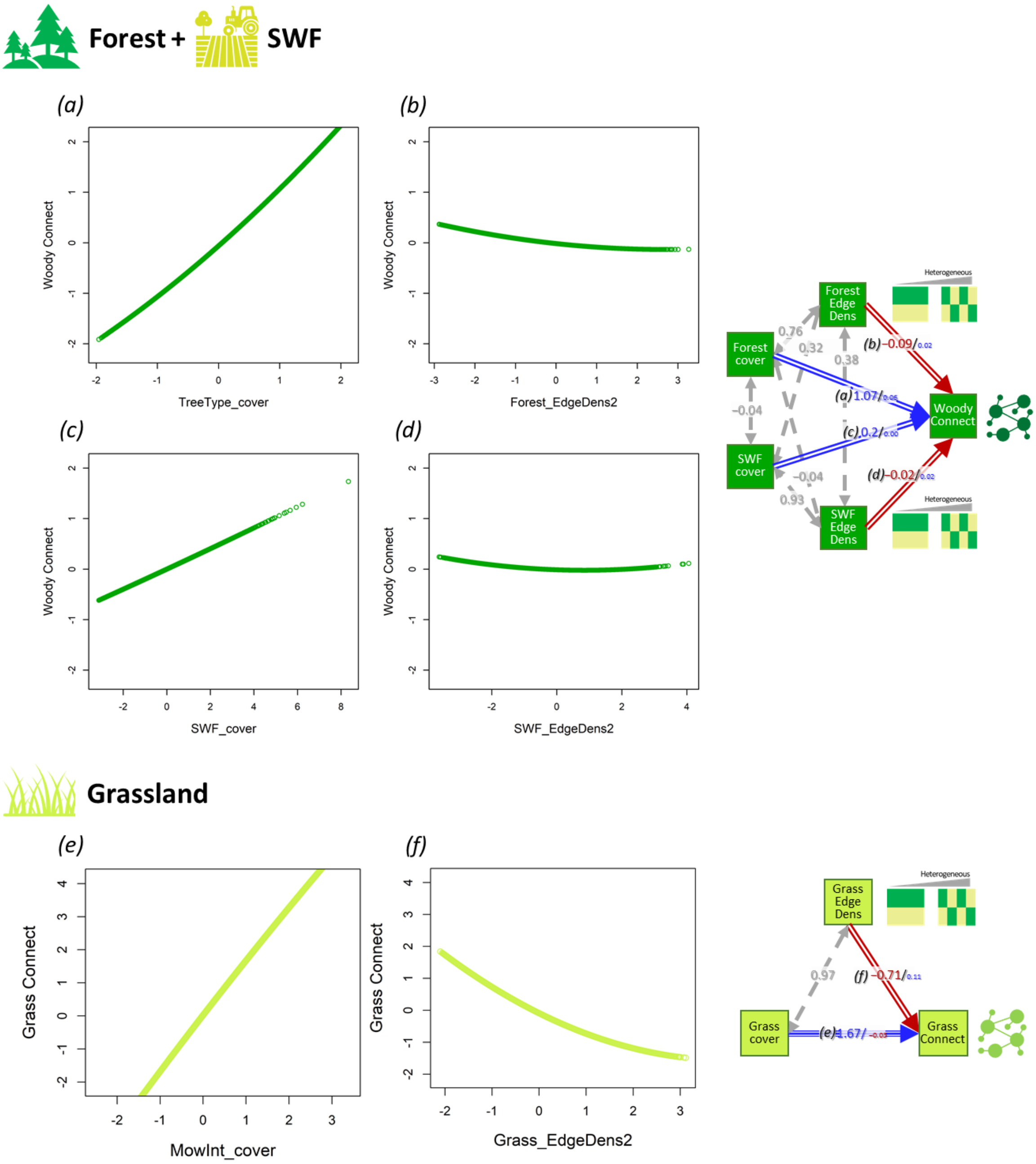

Figure S8. Relationship of partial regressions between predictors and response variables of each SEM in Fig. 4.

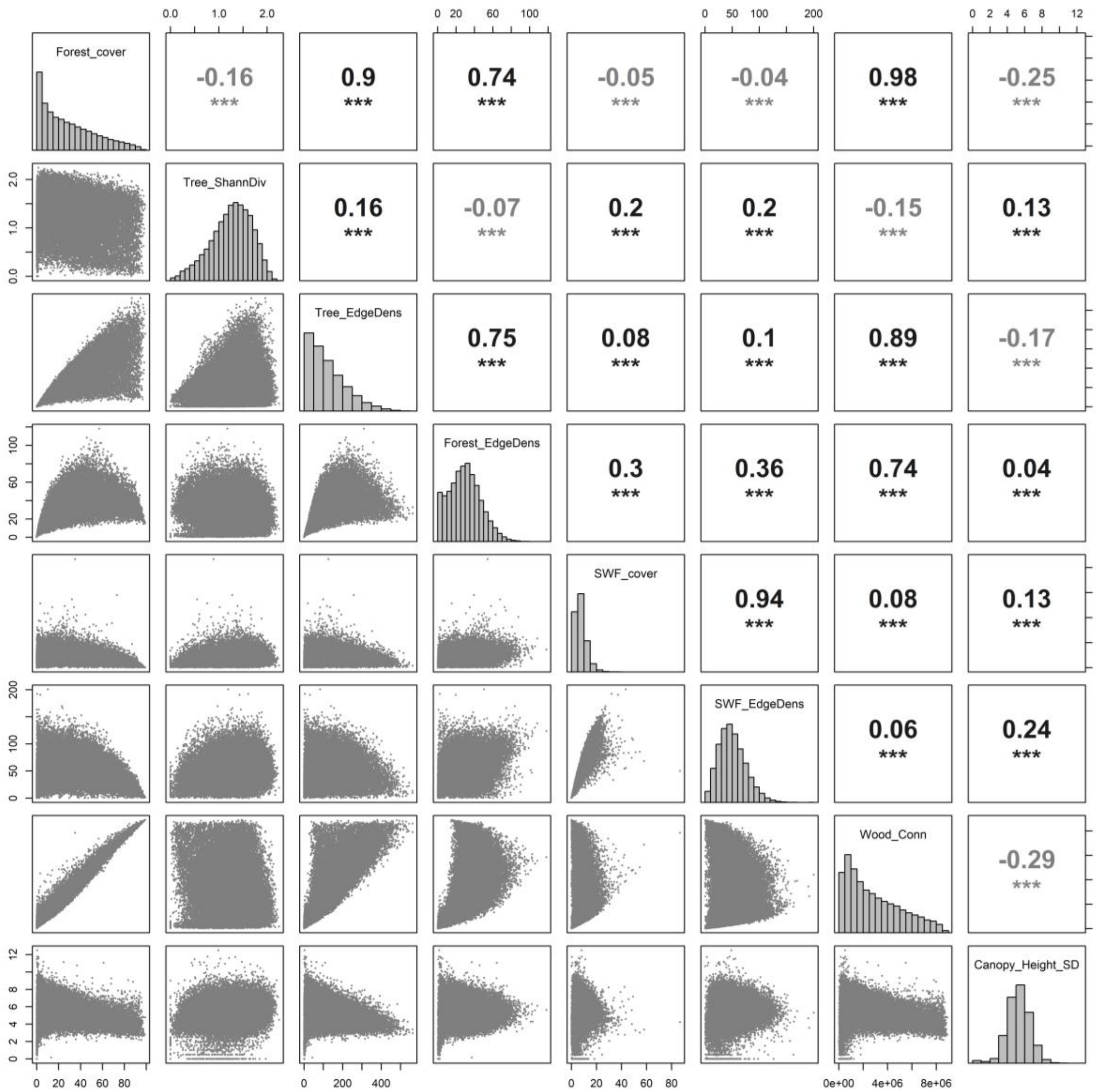

Figure S9. *Spearman*'s correlation between coverage, *H'*, ED, connectivity, and standard deviation of canopy height in forests.

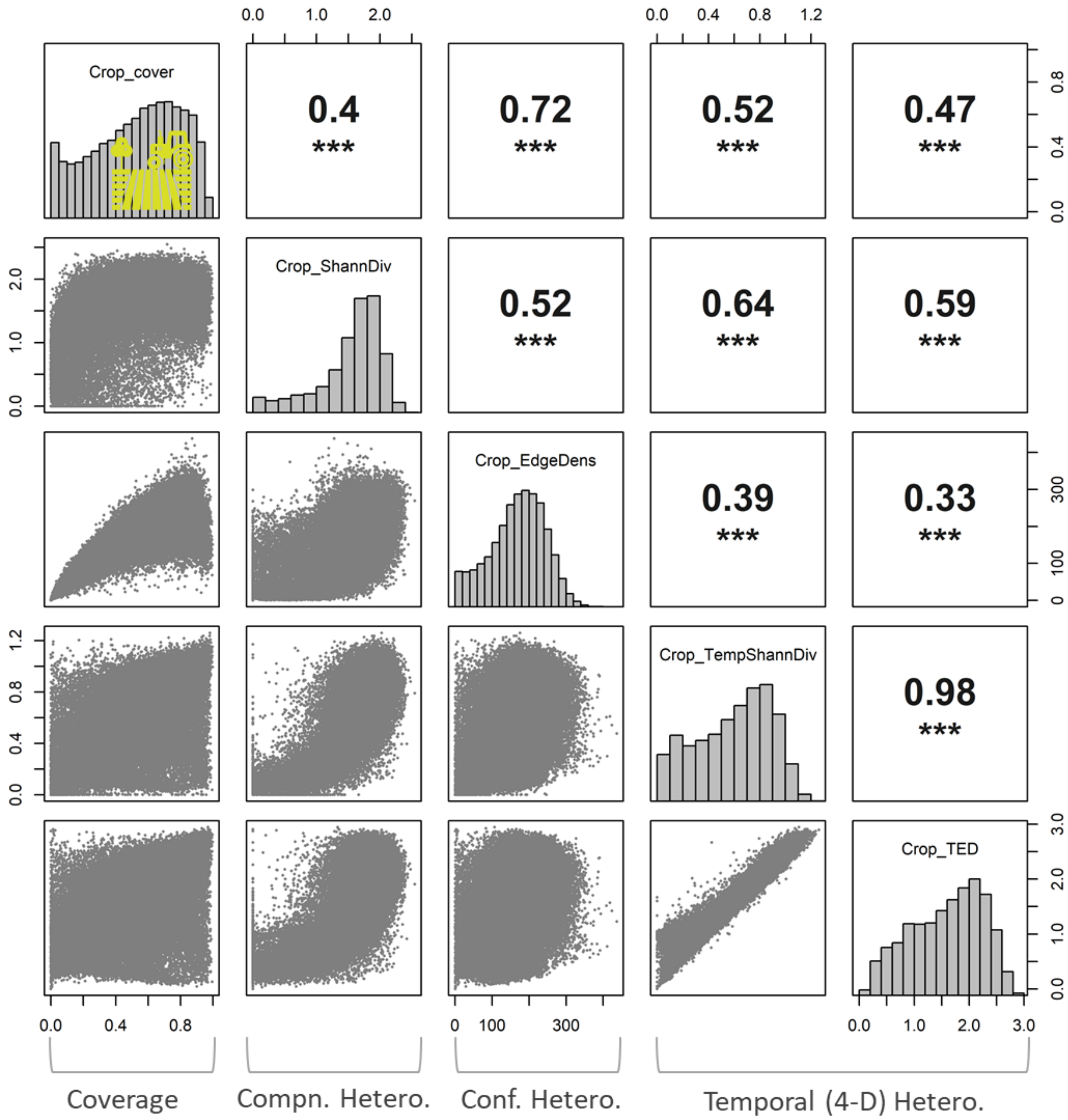

Figure S10. *Spearman*'s correlation between coverage, *H'*, ED, and temporal *H'*, temporal ED (interannual change rate) of crop types in croplands.

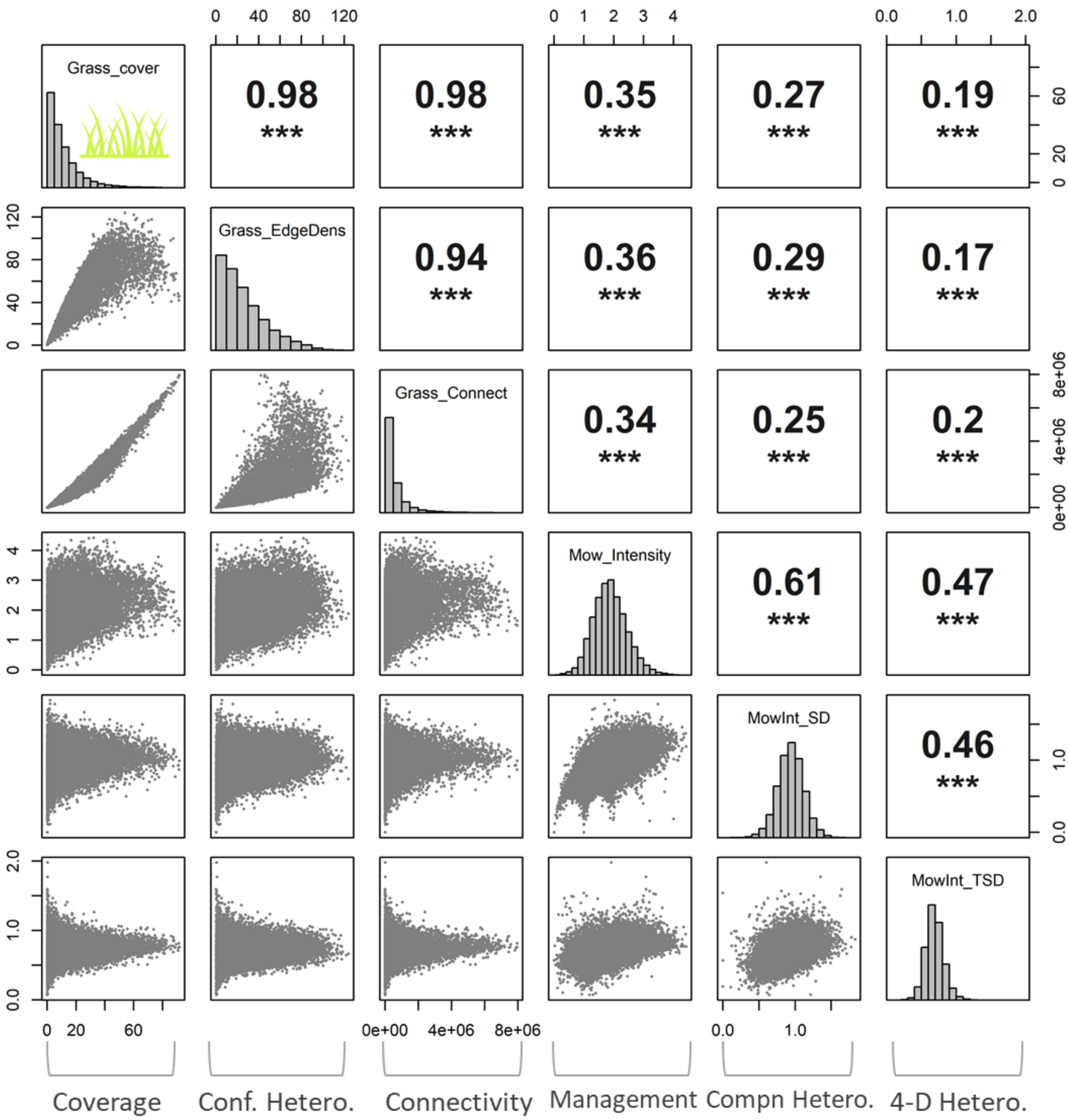

Figure S11. *Spearman*'s correlation between coverage, ED, connectivity, mean mowing frequency, *H'* and temporal *SD* of mowing frequency in grasslands.

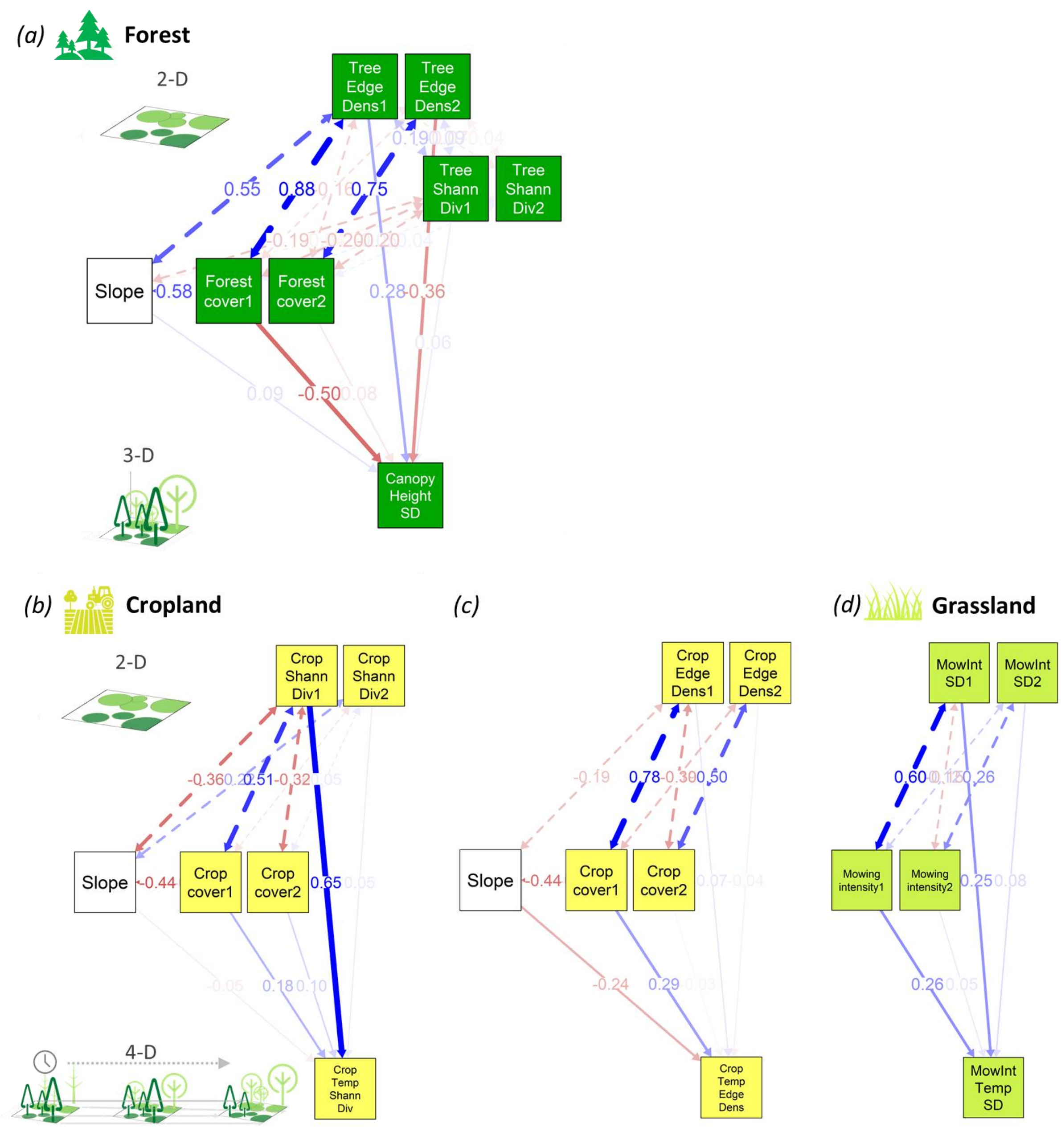

Figure S12. Full SEMS of Fig. 5 for the relationship between (a) horizontal *H'* and ED and vertical standard deviation (SD) in forests, (b) between horizontal and temporal *H'* and (c) between horizontal and temporal ED in croplands, and (d) horizontal and temporal SD in grasslands.

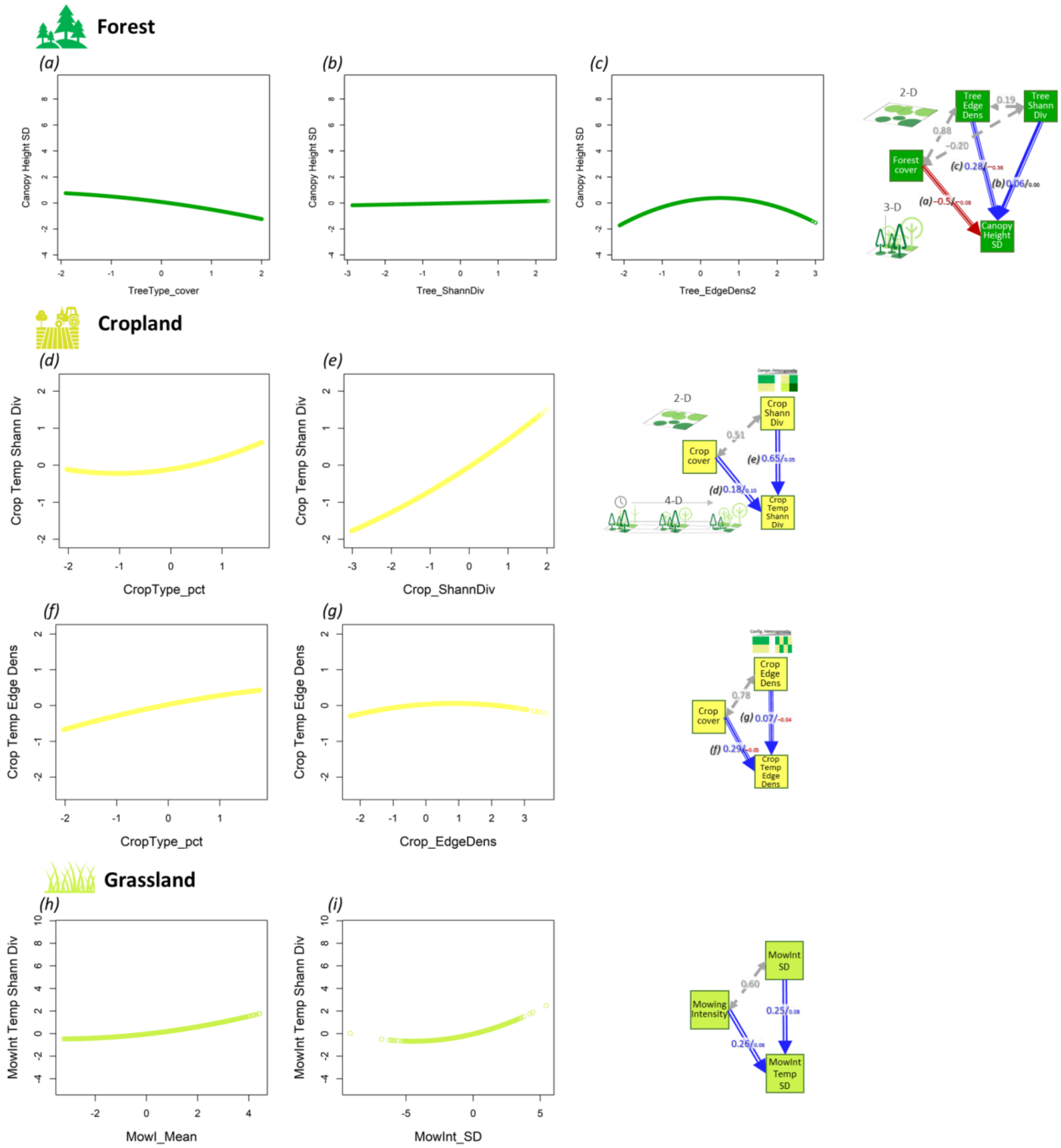

Figure S13. Relationship of partial regressions between predictors and response variables of each SEM in Fig. 5.

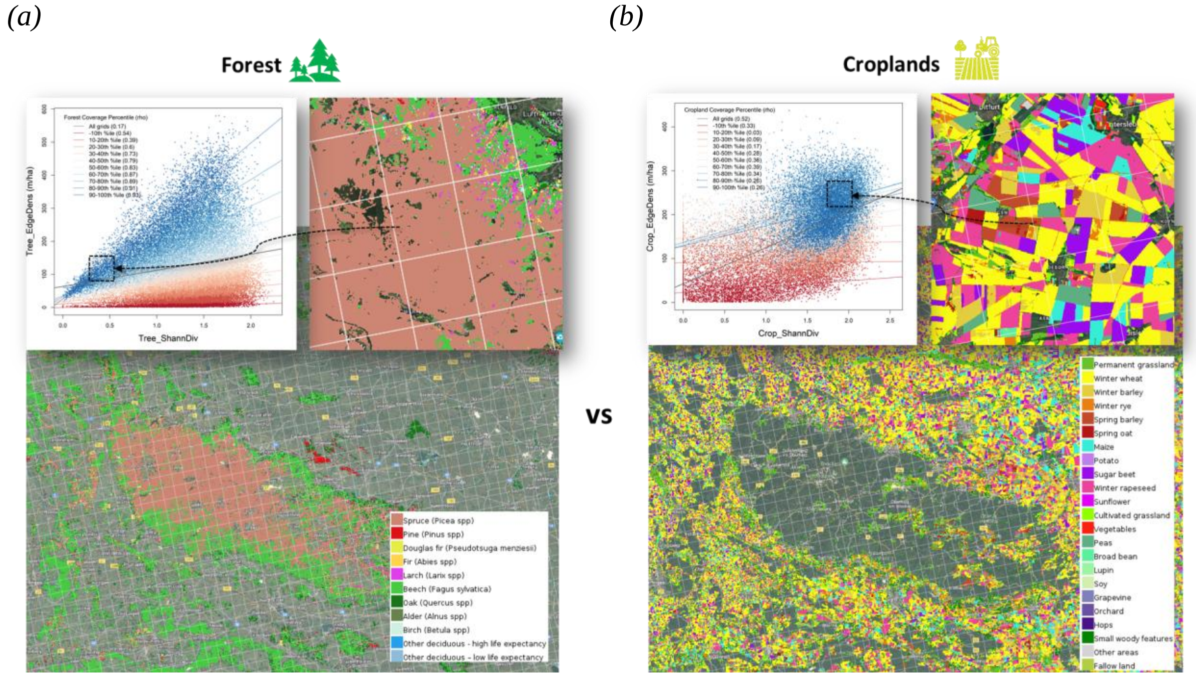

Figure S14. Comparison between (a) dominant tree type map and (b) crop type map in grid cells with high % forests and % croplands, respectively.

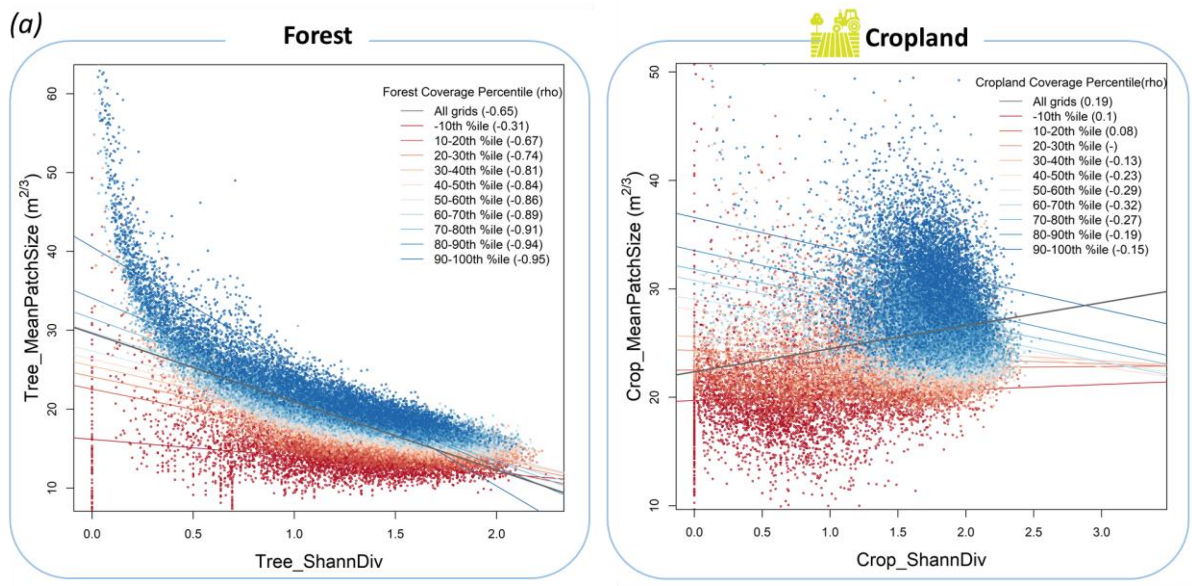

Figure S15. *Spearman*’s correlation between *H’* and mean patch size by deciles of coverage of (a) forests and (b) cropland. The mean patch size was transformed by cube root.

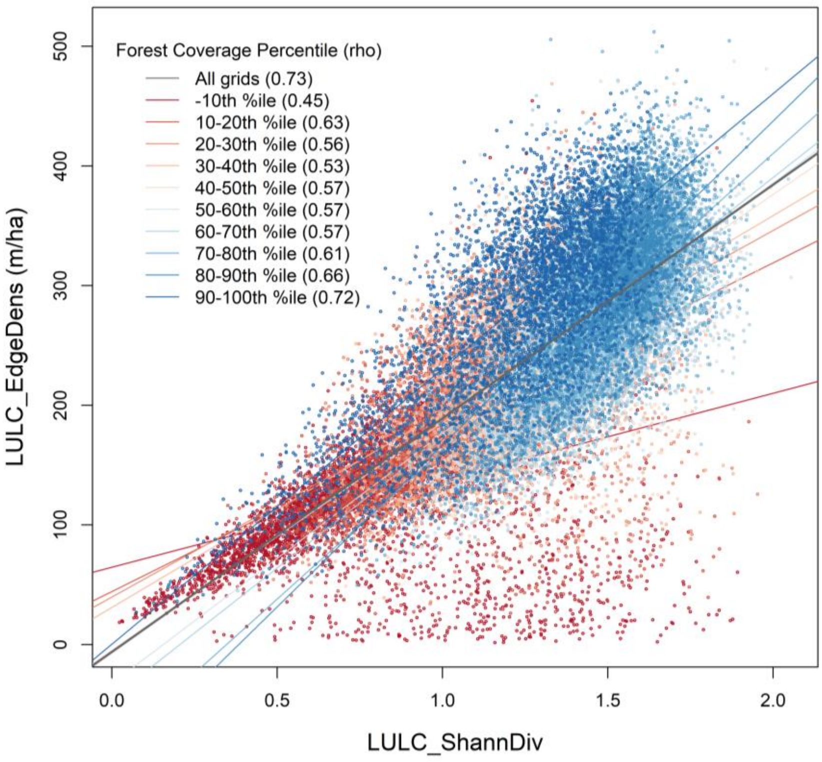

Figure S16. *Spearman*'s correlation between *H'* and ED of land-cover by deciles of % forest.

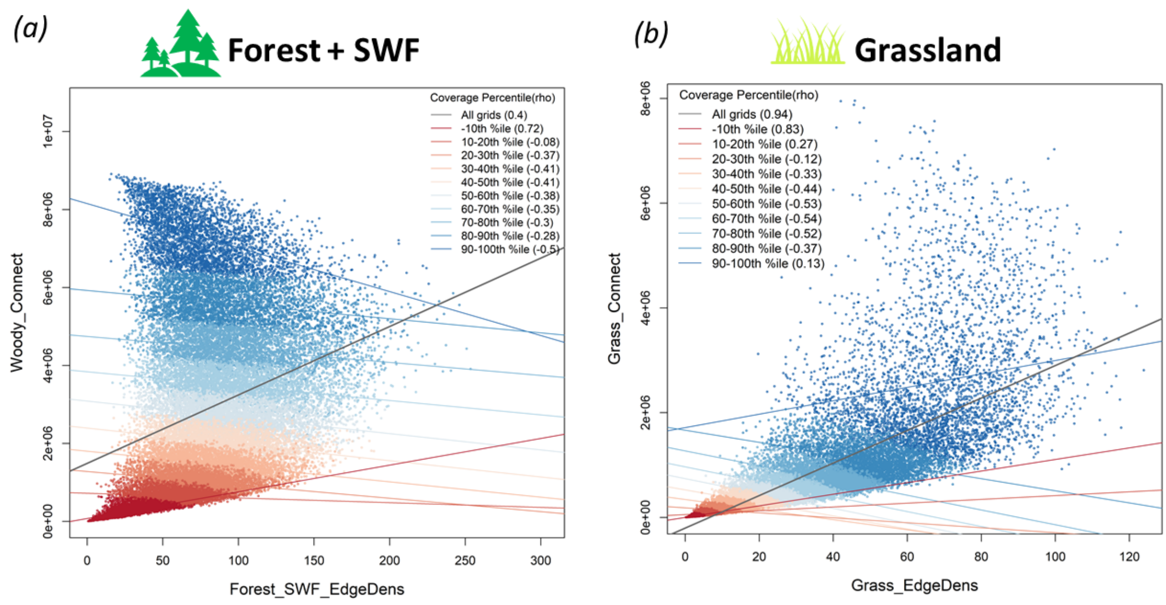

Figure S17. *Spearman*'s correlation between ED and connectivity by deciles of coverage of (a) forests and small woody features and (b) grasslands.

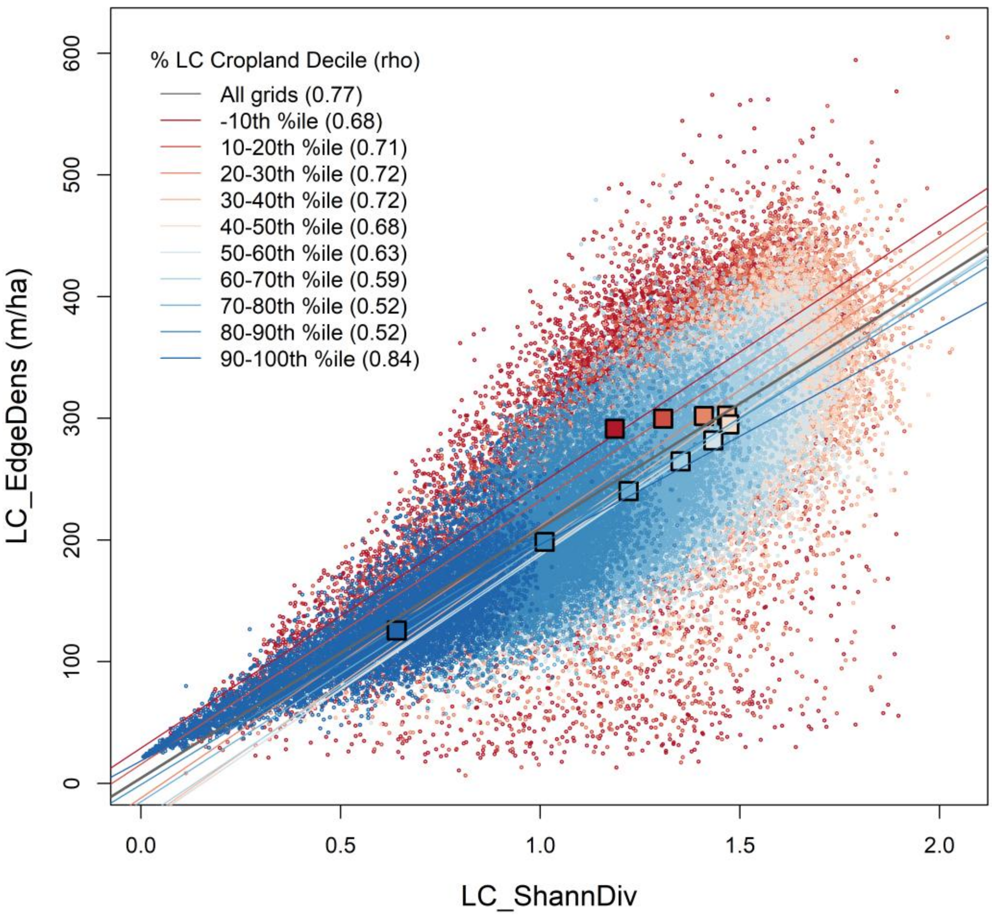

Figure S18. *Spearman*'s correlation between between *H'* and *ED* of all land-cover type with 2-km landscape grain.

Forest + SWF

(a)

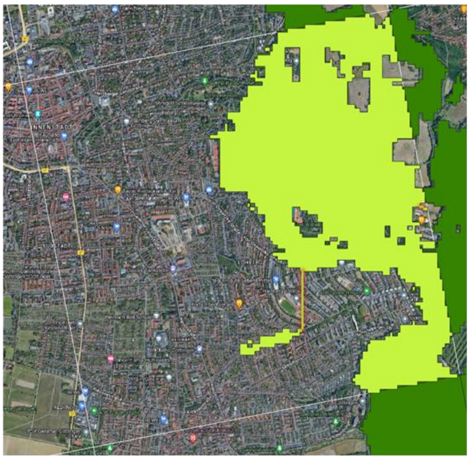

Edge density ↓ Connectivity ↑

Grid_id	% Habitat	ED	CONN
36897	31.5	32.8	2,807,344

(b)

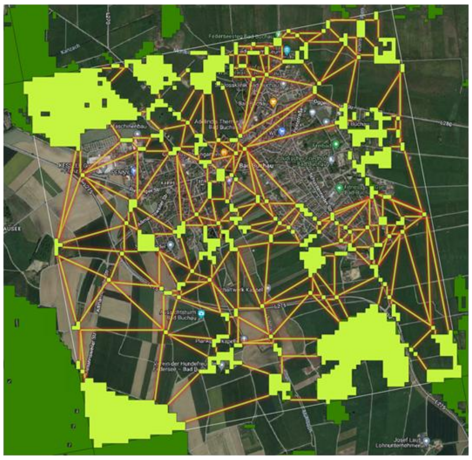

Edge density ↑ Connectivity ↓

Grid_id	% Habitat	ED	CONN
26000	26.5	89.4	1,061,337

Grassland

(c)

Edge density ↓ Connectivity ↑

Grid_id	% Habitat	ED	CONN
60853	7.9	7.6	670,331

(d)

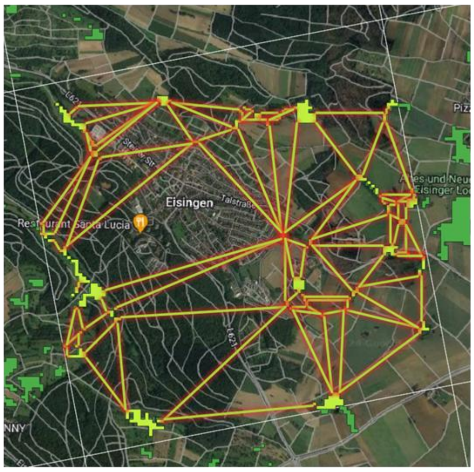

Edge density ↑ Connectivity ↓

Grid_id	% Habitat	ED	CONN
20619	5.9	19.6	137,201

Figure S19. Association between ED and connectivity.

(a) higher connectivity of woody features in landscapes with lower ED. (b) lower connectivity of woody features in landscapes with higher ED. % land-cover of woody features is similar in landscape (a) and (b) with a 40–50 percentile of % land-cover of woody features over Germany. (c) higher connectivity of grasslands in landscapes with lower ED. (d) lower connectivity of grasslands in landscapes with higher ED. % grasslands is similar in landscape (c) and (d) with a 40–50 percentile of % grasslands over Germany.

Land-cover

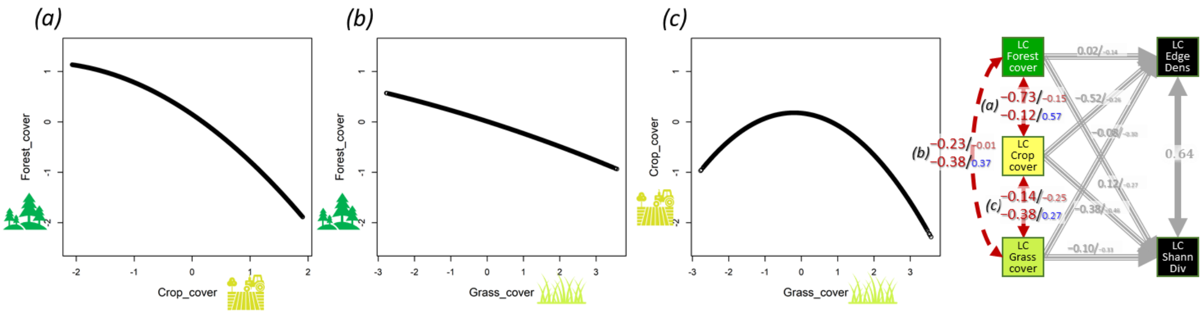

Figure S20. Partial correlation plots between % forests, % croplands, and % grasslands in SEM of Fig. 3.

Supplementary tables

Table S1. All abiotic factors before variable selection

	Subject	Metric	Data	Year	Res.
Topo	Elevation	Mean	SRTM DEM (NASA Shuttle Radar Topography Mission (SRTM) 2013)	2000	1 arc-second
	Slope	Mean			
Soil	Soil moisture	Mean	Daily soil moisture (Deutscher Wetterdienst (DWD) 2021)	1993-2022	1km
	Soil texture	PCA	Clay, sand, and silt contents (Hiederer 2013)	2006	1km
Climate	Annual Mean Temperature, maximum temperature of Warmest Month, minimum temperature of Coldest Month, Annual Precipitation, Precipitation of Wettest Month, Precipitation of Driest Month	Mean	WorldClim ver. 2 (Fick and Hijmans 2017)	1970-2000	30 seconds

Table S2. Parameter estimates for the structural equation models (SEMs) shown in Figures 3–5. Variables shown in grey indicate non-significant effects ($p \geq 0.05$).

Figure 3a				
Regressions:				
	Estimate	Std. Err	z-value	P(>|z|)
LC_ShannDiv	~			
SoilMoisture	-0.01	0.00	-1.72	0.09
Slope2	0.02	0.00	5.24	0.00
Forest_pct2_P1	0.12	0.01	22.92	0.00
Forest_pct2_P2	-0.28	0.00	-89.76	0.00
Crop_pct2_P1	-0.38	0.01	-81.19	0.00
Crop_pct2_P2	-0.46	0.00	-140.21	0.00
Grass_pct2_P1	-0.10	0.00	-25.52	0.00
Grass_pct2_P2	-0.33	0.00	-122.77	0.00
LC_EdgeDens	~			
SoilMoisture	0.15	0.00	35.08	0.00
Slope2	0.06	0.01	11.95	0.00
Forest_pct2_P1	0.02	0.01	2.95	0.00
Forest_pct2_P2	-0.14	0.01	-30.21	0.00
Crop_pct2_P1	-0.52	0.01	-74.63	0.00
Crop_pct2_P2	-0.26	0.01	-53.18	0.00
Grass_pct2_P1	-0.08	0.01	-15.27	0.00
Grass_pct2_P2	-0.30	0.00	-75.87	0.00
Covariances:				
	Estimate	Std. Err	z-value	P(>|z|)
.LC_ShannDiv	~~			

.LC_EdgDns	0.19	0.00	104.95	0.00

Variances:

	Estimate	Std. Err	z-value	P(>|z|)
.LC_ShnnDv	0.20	0.00	138.24	0.00
.LC_EdgDns	0.44	0.00	138.24	0.00

R-Square:

	Estimate
LC_ShnnDv	0.80
LC_EdgDns	0.56

Figure 3c

Regressions:

	Estimate	Std. Err	z-value	P(>|z|)
Tree_EdgeDens2	~			
Slope2	0.06	0.00	20.24	0.00
TreeTyp_pct2_P1	0.85	0.00	312.62	0.00
TreeTyp_pct2_P2	-0.16	0.00	-70.68	0.00
Tree_ShannDiv	~			
Slope2	-0.12	0.01	-20.14	0.00
TreeTyp_pct2_P1	-0.12	0.01	-20.35	0.00
TreeTyp_pct2_P2	-0.21	0.01	-44.00	0.00

Covariances:

	Estimate	Std. Err	z-value	P(>|z|)
.Tree_EdgeDens2	~~			
.Tree_ShannDiv	0.34	0.00	123.97	0.00

Variances:

	Estimate	Std. Err	z-value	P(>|z|)
.Tree_EdgeDens2	0.20	0.00	141.24	0.00
.Tree_ShannDiv	0.91	0.01	141.24	0.00

R-Square:

	Estimate
Tree_EdgeDens2	0.80
Tree_ShannDiv	0.09

Figure 3e

Regressions:

	Estimate	Std. Err	z-value	P(>|z|)
Crop_EdgeDens	~			
Slope2	0.14	0.00	46.51	0.00
CropTyp_pct_P1	0.84	0.00	286.17	0.00
CropTyp_pct_P2	-0.28	0.00	-102.63	0.00
Crop_ShannDiv	~			

Slope2	-0.24	0.00	-54.45	0.00
CropTyp_pct_P1	0.41	0.00	94.67	0.00
CropTyp_pct_P2	-0.36	0.00	-91.54	0.00
Covariances:				
	Estimate	Std. Err	z-value	P(>|z|)
.Crop_EdgeDens	~~			
.Crop_ShannDiv	0.10	0.00	49.04	0.00
Variances:				
	Estimate	Std. Err	z-value	P(>|z|)
.Crop_EdgeDens	0.28	0.00	142.96	0.00
.Crop_ShannDiv	0.60	0.00	142.96	0.00
R-Square:				
	Estimate			
Crop_EdgeDens	0.72			
Crop_ShannDiv	0.40			
Figure 4a				
Regressions:				
	Estimate	Std. Err	z-value	P(>|z|)
CI_EC2	~			
Slope2	-0.01	0.00	-14.59	0.00
TreeTyp_pct2_P1	1.07	0.00	873.28	0.00
TreeTyp_pct2_P2	0.06	0.00	78.10	0.00
Frst_EdgDn2_P1	-0.10	0.00	-72.60	0.00
Frst_EdgDn2_P2	0.02	0.00	31.39	0.00
SWF_pct2_P1	0.20	0.00	124.89	0.00
SWF_pct2_P2	0.00	0.00	1.63	0.10
SWF_EdgDns2_P1	-0.02	0.00	-13.78	0.00
SWF_EdgDns2_P2	0.02	0.00	22.49	0.00
Variances:				
	Estimate	Std. Err	z-value	P(>|z|)
.CI_EC2	0.01	0.00	137.59	0.00
R-Square:				
	Estimate			
CI_EC2	0.99			
Figure 4b				
Regressions:				
	Estimate	Std. Err	z-value	P(>|z|)
Grass_CI2	~			
SoilMoisture	0.00	0.00	-1.54	0.12
MowInt_pct2_P1	1.67	0.00	579.41	0.00

MowInt_pct2_P2	-0.03	0.00	-24.10	0.00
Grss_EdgDn2_P1	-0.71	0.00	-240.29	0.00
Grss_EdgDn2_P2	0.11	0.00	76.56	0.00

Variances:

	Estimate	Std. Err	z-value	P(>|z|)
.Grass_CI2	0.01	0.00	135.04	0.00

R-Square:

	Estimate
Grass_CI2	0.99

Figure 5a

Regressions:

	Estimate	Std. Err	z-value	P(>|z|)
CHM_SD	~			
Slope2	0.09	0.01	16.56	0.00
TreeTyp_pct2_P1	-0.50	0.03	-19.84	0.00
TreeTyp_pct2_P2	-0.08	0.01	-7.10	0.00
Tree_EdgDns2_P1	0.28	0.03	10.78	0.00
Tree_EdgDns2_P2	-0.36	0.01	-34.06	0.00
Tree_ShnnDv_P1	0.06	0.01	6.83	0.00
Tree_ShnnDv_P2	0.00	0.01	0.31	0.76

Variances:

	Estimate	Std. Err	z-value	P(>|z|)
.CHM_SD	0.76	0.01	140.99	0.00

R-Square:

	Estimate
CHM_SD	0.24

Figure 5b

Regressions:

	Estimate	Std. Err	z-value	P(>|z|)
Crop_TDiv	~			
Slope2	-0.05	0.00	-11.73	0.00
CropTyp_pct_P1	0.19	0.00	46.52	0.00
CropTyp_pct_P2	0.11	0.00	28.90	0.00
Crop_ShnnDv_P1	0.65	0.00	154.04	0.00
Crop_ShnnDv_P2	0.05	0.00	14.42	0.00

Variances:

	Estimate	Std. Err	z-value	P(>|z|)
.Crop_TDiv	0.43	0.00	142.94	0.00

R-Square:

	Estimate			
Crop_TDiv	0.58			
Figure 5c				
Regressions:				
	Estimate	Std. Err	z-value	P(>|z|)
MowInt_TDiv	~			
MowI_Mean_P1	0.23	0.01	37.98	0.00
MowI_Mean_P2	0.04	0.01	9.16	0.00
MwInt_ShnnD_P1	0.25	0.01	41.13	0.00
MwInt_ShnnD_P2	0.04	0.01	8.67	0.00
Variances:				
	Estimate	Std. Err	z-value	P(>|z|)
.MowInt_TDiv	0.81	0.01	139.97	0.00
R-Square:				
	Estimate			
MowInt_TDiv	0.19			

Table S3. Description of variables in SEMs in Figures 3-5. All variables in SEMs are described with their labels in Figures 3-5, variable names in Table S1, and transformation due to skewness of data distribution.

Fig	Label in Figures	Variable in Table S1	Description	Transformation
Fig. 3a	Soil Moist	SoilMoisture	Mean soil moisture	-
	Slope	Slope2	Mean slope	Square root
		Forest_pct2	Percentage of forests in LC map	
	LC Forest cover1	Forest_pct2_P1	Orthogonal first-order polynomial of Forest_pct2	Square root
	LC Forest cover2	Forest_pct2_P2	Orthogonal second-order polynomial of Forest_pct2	
		Crop_pct2	Percentage of croplands in LC map	
	LC Crop cover1	Crop_pct2_P1	Orthogonal first-order polynomial of Crop_pct2	Square root
	LC Crop cover2	Crop_pct2_P2	Orthogonal second-order polynomial of Crop_pct2	
		Grass_pct2	Percentage of grasslands in LC map	
	LC Grass cover1	Grass_pct2_P1	Orthogonal first-order polynomial of Grass_pct2	Square root
	LC Grass cover2	Grass_pct2_P2	Orthogonal second-order polynomial of Grass_pct2	
	LC EdgeDens	LC_EdgeDens	Edge density of LC map	-
	LC ShannDiv	LC_ShannDiv	Shannon diversity of LC map	-
Fig. 3c		TreeTyp_pct2	Percentage of forests in the forest map	
	Forest cover1	TreeTyp_pct2_P1	Orthogonal first-order polynomial of TreeTyp_pct2	Square root
	Forest cover2	TreeTyp_pct2_P2	Orthogonal second-order polynomial of TreeTyp_pct2_P1	

	Tree EdgeDens	Tree_EdgeDens2	Edge density of dominant forest tree species map	Square root
	Tree ShannDiv	Tree_ShannDiv	Shannon diversity of dominant forest tree species map	-
Fig. 3e		CropTyp_pct	Percentage of croplands in crop type map	-
	Crop cover1	CropTyp_pct_P1	Orthogonal first-order polynomial of CropTyp_pct_P1	
	Crop cover2	CropTyp_pct_P2	Orthogonal second-order polynomial of CropTyp_pct_P1	
	Crop EdgeDens	Crop_EdgeDens	Edge density of crop type map	-
	Crop ShannDiv	Crop_ShannDiv	Shanno diversity of crop type map	-
Fig. 4a		Frst_EdgDn2	Edge density of forest in the forest map	Square root
	Forest EdgeDens1	Frst_EdgDn2_P1	Orthogonal first-order polynomial of Frst_EdgDn2	
	Forest EdgeDens2	Frst_EdgDn2_P2	Orthogonal second-order polynomial of Frst_EdgDn2	
		SWF_pct2	Percentage of small woody features in crop type map	Square root
	SWF cover1	SWF_pct2_P1	Orthogonal first-order polynomial of SWF_pct2	
	SWF cover2	SWF_pct2_P2	Orthogonal second-order polynomial of SWF_pct2	
		SWF_EdgDns2	Edge density of small woody features in the crop-type map	Square root
	SWF EdgeDens1	SWF_EdgDns2_P1	Orthogonal first-order polynomial of SWF_EdgDns2	
	SWF EdgeDens2	SWF_EdgDns2_P2	Orthogonal second-order polynomial of SWF_EdgDns2	
	Woody Connect	CI_EC2	Woody connectivity index of forests and small woody features	Square root
Fig. 4b		MowInt_pct2	Percentage of grasslands in mowing frequency map	Cube root
	Grass cover1	MowInt_pct2_P1	Orthogonal first-order polynomial of MowInt_pct2	
	Grass cover2	MowInt_pct2_P2	Orthogonal second-order polynomial of MowInt_pct2	
		Grss_EdgDn2	Edge density of grasslands in mowing frequency map	Square root
	Grass EdgeDens1	Grss_EdgDn2_P1	Orthogonal first-order polynomial of Grss_EdgDn2	
	Grass EdgeDens2	Grss_EdgDn2_P2	Orthogonal second-order polynomial of Grss_EdgDn2	
	Grass Connect	Grass_CI2	Grassland connectivity index of grasslands	Cube root
Fig. 5a	Tree EdgeDens1	Tree_EdgDns2_P1	Orthogonal first-order polynomial of Tree_EdgeDens2	
	Tree EdgeDens2	Tree_EdgDns2_P2	Orthogonal second-order polynomial of Tree_EdgeDens2	
	Tree ShannDiv1	Tree_ShnnDv_P1	Orthogonal first-order polynomial of Tree_ShannDiv	
	Tree ShannDiv2	Tree_ShnnDv_P2	Orthogonal second-order polynomial of Tree_ShannDiv	
	Canopy Height SD	CHM_SD	Standard deviation of canopy height model	-
Fig. 5b	Crop TempShannDiv	Crop_TDiv	Temporal Shannon diversity of crop type map across 4 years	
	Crop ShannDiv1	Crop_ShnnDv_P1	Orthogonal first-order polynomial of Crop_ShannDiv	

	Crop ShannDiv2	Crop_ShnnDv_P2	Orthogonal second-order polynomial of Crop_ShannDiv
Fig . 5c	MowInt TempShannDiv	MowInt_TDiv	Temporal Shannon diversity of mowing intensities across 4 years
		MowI_Mean	Mean mowing frequency
	Mowing intensity1	MowI_Mean_P1	Orthogonal first-order polynomial of MowI_Mean
	Mowing intensity2	MowI_Mean_P2	Orthogonal second-order polynomial of MowI_Mean
		MwInt_ShnnD	Shannon diversity of mowing frequency map
	MowInt ShannDiv1	MwInt_ShnnD_P1	Orthogonal first-order polynomial of MwInt_ShnnD
	MowInt ShannDiv2	MwInt_ShnnD_P2	Orthogonal second-order polynomial of MwInt_ShnnD

Table S4. Importance of components of principal component analysis (PCA) to explore datasets of horizontal, vertical, and temporal landscape heterogeneity indices.

	PC1	PC2	PC3	PC4	PC5
Eigenvalue	4.38	2.70	2.02	1.26	1.06
Proportion Explained	0.29	0.18	0.13	0.09	0.08
Cumulative Proportion	0.29	0.47	0.61	0.69	0.76

Table S5. Coordinates of the arrowheads of horizontal, vertical, and temporal landscape heterogeneity indices

	PC1	PC2	PC3	PC4	PC5
DomTree_ShannDiv	-0.69	-0.01	-3.63	-1.22	5.06
DomTree_EdgeDens	5.60	-2.12	-1.53	-1.12	1.67
Wood_Conn	5.95	-2.29	0.63	-0.91	-0.25
Canopy_Height_SD	-2.24	1.57	-2.83	0.57	0.46
Crop_ShannDiv	-4.27	-1.46	-3.53	0.18	-0.73
Crop_EdgeDens	-3.78	2.49	-3.85	1.85	-1.00
Avg_FarmSize	-3.70	-0.96	1.29	-1.96	3.50
Crop_TempShannDiv	-5.37	-3.33	-1.80	-0.70	-0.75
Grass_EdgeDens	1.22	6.30	-0.37	1.50	0.91
Grass_Conn	0.66	5.87	1.89	0.95	1.74
MowInt_ShannDiv	0.33	4.00	-1.62	-3.59	-2.17
MowInt_TempShannDiv	-0.54	2.60	-0.41	-5.67	-0.98
LC_ShannDiv	4.05	-0.52	-4.44	0.18	-0.18
LC_EdgeDens	4.74	0.29	-4.43	0.80	-0.55

Table S6. Coverage ranges (% land-cover) of 3 × 3 km grids for each decile for quantile correlation between H’ and ED of (a) land-cover types, (b) forest, and (c) croplands

(a)

Percentile (n=39,991)	**Cropland coverage**
Under 10th	0 – 1.4%
10th – 20th	1.4 – 6.6%
20th – 30th	6.6 – 13.8%
30th – 40th	13.8 – 21.5%
40th – 50th	21.5 – 29.4%
50th – 60th	29.4 – 37.4%
60th – 70th	37.4 – 46.2%
70th – 80th	46.2 – 55.8%
80th – 90th	55.8 – 68.5%
90th – 100th	68.5 – 99.5%

(b)

Percentile (n=39,894)	**Forest coverage**
Under 10th	0 – 5.8%
10th – 20th	5.8 – 11.3%
20th – 30th	11.3 – 16.9%
30th – 40th	16.9 – 23%
40th – 50th	23 – 30%
50th – 60th	30 – 38%
60th – 70th	38 – 47.4%
70th – 80th	47.4 – 59.2%
80th – 90th	59.2 – 75.4%
90th – 100th	75.4 – 99.8%

(c)

Percentile (n=39,976)	**Cropland coverage**
Under 10th	0 – 1.4%
10th – 20th	1.4 – 6.7%
20th – 30th	6.7 – 13.9%
30th – 40th	13.9 – 21.5%
40th – 50th	21.5 – 29.4%
50th – 60th	29.4 – 37.4%
60th – 70th	37.4 – 46.2%
70th – 80th	46.2 – 55.8%
80th – 90th	55.8 – 68.5%
90th – 100th	68.5 – 99.5%

Supplementary notes

Note S1. Equations of *Shannon* diversity index (*H'*) and edge density (*ED*)

$$Shannon\ diversity\ index\ (H') = -\sum_{i=1}^{S} p_i \ln p_i$$

S = total number of land-cover types

p_i = Proportion covered by land-cover type i

$$Edge\ density\ (ED) = \frac{E}{A}$$

E = total length of all edge segments (in meters)

A = total landscape area of a 3 x 3 km grid cell (900 ha)

References

1. Blickensdörfer L, Oehmichen K, Pflugmacher D, et al (2024) National tree species mapping using Sentinel-1/2 time series and German National Forest Inventory data. Remote Sensing of Environment 304:114069. https://doi.org/10.1016/j.rse.2024.114069
2. Blickensdörfer L, Schwieder M, Pflugmacher D, et al (2022) Mapping of crop types and crop sequences with combined time series of Sentinel-1, Sentinel-2 and Landsat 8 data for Germany. Remote Sensing of Environment 269:112831. https://doi.org/10.1016/j.rse.2021.112831
3. Deutscher Wetterdienst (DWD) (2021) Daily grids of soil moisture under grass for Germany, Version v2.0
4. Federal Statistical Office and the statistical offices of the Länder (2020) Atlas Agrarstatistik
5. Fick SE, Hijmans RJ (2017) WorldClim 2: new 1-km spatial resolution climate surfaces for global land areas. International Journal of Climatology 37:4302–4315. https://doi.org/10.1002/joc.5086
6. Hiederer R (2013) Mapping Soil Properties for Europe – Spatial Representation of Soil Database Attributes. Publications Office of the European Union, Luxembourg
7. Lang N, Jetz W, Schindler K, Wegner JD (2022) A high-resolution canopy height model of the Earth
8. NASA Shuttle Radar Topography Mission (SRTM) (2013) Shuttle Radar Topography Mission (SRTM) Global. Distributed by OpenTopography
9. Pflugmacher D, Rabe A, Peters M, Hostert P (2018) Pan-European land cover map of 2015 based on Landsat and LUCAS data. Supplement to: Pflugmacher, D et al. (2019): Mapping pan-European land cover using Landsat spectral-temporal metrics and the European LUCAS

survey. Remote Sensing of Environment, 221, 583-595, https://doi.org/10.1016/j.rse.2018.12.001

10. Saura S, Estreguil C, Mouton C, Rodríguez-Freire M (2011) Network analysis to assess landscape connectivity trends: Application to European forests (1990–2000). Ecological Indicators 11:407–416. https://doi.org/10.1016/j.ecolind.2010.06.011

11. Schwieder M, Wesemeyer M, Frantz D, et al (2022) Mapping grassland mowing events across Germany based on combined Sentinel-2 and Landsat 8 time series. Remote Sensing of Environment 269:112795. https://doi.org/10.1016/j.rse.2021.112795